Theory of the pseudogap state of the cuprates

C. M. Varma
Physics Department, University of California, Riverside, California 92507, USA
(Received 22 July 2005; revised manuscript received 8 November 2005; published 18 April 2006)

The phase diagram for a general model for cuprates is derived in a mean-field approximation. A phase-violating time reversal without breaking translational symmetry is possible when both the ionic interactions and the local repulsions are large compared to the energy difference between the Cu and O single-particle levels. It ends at a quantum critical point as the hole or electron doping is increased. Such a phase is necessarily accompanied by singular forward scattering such that, in the stable phase, the density of states at the chemical potential, projected to a particular point-group symmetry of the lattice is zero, producing thereby an anisotropic gap in the single-particle spectrum. It is suggested that this phase occupies the "pseudogap" region of the phase diagram of the cuprates. The temperature dependence of the single-particle spectra, the density of states, the specific heat, and the magnetic susceptibility are calculated with rather remarkable correspondence with the experimental results. The importance of further direct experimental verification of such a phase in resolving the principal issues in the theory of the cuprate phenomena is pointed out. To this end, some predictions are provided.

DOI: 10.1103/PhysRevB.73.155113 PACS number(s): 71.10.−w, 74.20.−z

I. INTRODUCTION

It became quickly apparent following the initial discovery[1] that the high superconducting transition temperatures in the cuprates were not the only interesting feature of these compounds. The properties in the normal state(s) are unlike those of other metals and new concepts are required to understand them. Moreover, the superconductivity can be understood only if they are understood since the fluctuations responsible for the superconducting instability are a property of the normal state.

The extensive investigation of the cuprates[2,3] has led to a consistent set of experimental results from which a universal phase diagram, Fig. 1, for these compounds was drawn,[4–6] and for which considerable further evidence has been adduced.[3,7–10] This diagram was drawn on the basis of the measured properties, thermodynamic as well as transport, which show characteristic changes across the lines drawn in all the cuprates. A fundamental aspect of the phase diagram is the existence of a putative quantum critical point (QCP) inside the regime of compositions for superconductivity. Besides the superconducting region, there lie, as marked in Fig. 1, three distinct regions emanating from the QCP. This paper is concerned primarily with region II of the phase diagram, but as explained below, its nature is tied to the nature of the QCP and the fluctuations above it and understanding it amounts to understanding the essentials of the physics of the cuprate phenomena.

In previous work,[4,5] a broken time-reversal symmetry due to orbital current fluctuations, without altering the translational symmetry (circulating current phases), has been derived for region II. Such a broken symmetry has been inferred in polarized angle-resolved photoemission experiments.[11] Recently, direct magnetic diffraction experiments using polarized neutron diffraction experiments[12] have observed a broken symmetry consistent with the predictions. The principal aim of this paper is to give the details of the physics and calculations of the previous work[4–6] and to discuss several additional related issues. A detailed theory of the anisotropic gap accompanying the time-reversal breaking is presented and equilibrium thermodynamic properties are calculated and compared with experiments.

Quantum critical point. The QCP was anticipated by the marginal Fermi-liquid hypothesis,[13] which proposed a scale-invariant spectrum of fluctuations to explain the normal state properties in region I and led to a set of predictions for the single-particle spectra and transport properties which have been verified.[14–16] The suggestion[13] that the same spectrum provides a glue for superconductive pairing is also consistent with that deduced from approximate inversion of angle-resolved photoemission (ARPES) data[17] in the superconductive state. The proposed spectrum of quantum critical fluctuations has an absorptive part,

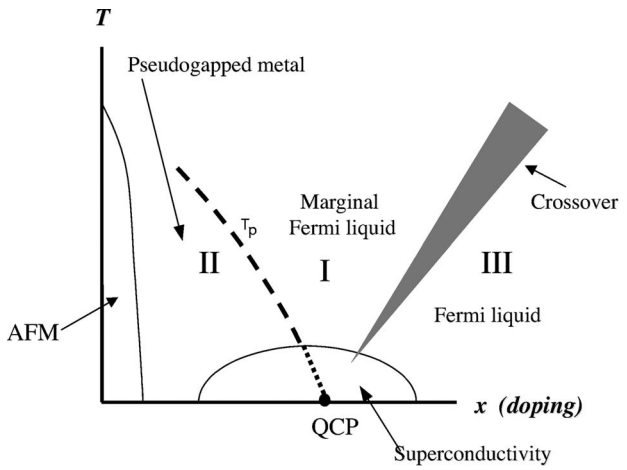

FIG. 1. A schematic of the universal phase diagram for the cuprates; the lines shown and the crossover occur in all the cuprate compounds. Other features, small regions of antiferromagnetism away from half filling, charge-density modulations, stripes, etc., that occur in one or the other cuprates as well as the spin-glass region are not shown.

$$\mathrm{Im}\,\chi(\mathbf{q},\omega,T) \propto \begin{cases} \omega/T & \text{for } \omega \ll T, \\ \text{const} & \text{for } T \ll \omega \ll \omega_c, \end{cases} \quad (1)$$

where ω_c is a cutoff, determinable from experiments. The corresponding real part of the fluctuations is $\mathrm{Re}\,\chi(\mathbf{q},\omega,T) \propto \ln(\omega_c/\omega)$ for $\omega/T \gg 1$ and $\propto \ln(\omega_c/T)$ for $\omega/T \ll 1$. Phenomenology[13] does not specify what operator has fluctuations of this form. The microscopic theory in this paper provides the answer that the spectra are the fluctuations which condense to form the broken symmetry in region II and are therefore of current fluctuations in a particular irreducible representation of the lattice.

It is characteristic of QCP's in itinerant fermions[18,19] that a crossover to a Fermi liquid is expected characterized by a line emanating from $x=x_c$. Below another line emanating from $x=x_c$, a broken symmetry is expected. These expectations are consistent with the experimental phase diagram of Fig. 1: characteristic Fermi-liquid properties are found deep in region III and in region II an anisotropic gap (pseudogap) in the one-particle spectra at the chemical potential is observed.[20] Transport[10] and thermodynamic properties[21,22] also show characteristic changes below the line $T_p(x)$. However, the nature of region II remains in doubt. There is plenty of empirical evidence to conclude that region II does not universally break translational and/or spin-rotational symmetries. If it is a phase of broken symmetry, it is of an unusual nature.

Region II of the phase diagram. A knowledge of the ground state and excitations of region II ties together every essential aspect of the cuprate problem. Given a QCP, region III follows automatically. Given the success of the predictions following from the phenomenological spectrum of Eq. (1), one can be reasonably certain about the functional form of the spectrum. Since the broken symmetry in region II is due to the condensation of the fluctuations in region I, a knowledge of the former specifies the nature of the latter. It answers the question as to the fluctuations of which operator have the spectrum given by Eq. (1). There is experimental evidence[17] that Eq. (1) also gives the glue for the pairing instability for superconductivity. Therefore a knowledge of region II specifies the pairing mechanism as well.

A hint is available about the possible broken symmetry in region II from the Raman spectra, which measures the $q \to 0$ part of the particle-hole fluctuations in even-parity point-group symmetries. In region I, it is firmly established that the spectrum is consistent[23] with the predicted form Eq. (1). For conserved quantities like the density or spin density, the correlation functions must be proportional to q^2 at small q. Therefore one infers that the observed singularity is in the correlation function of an unconserved operator in some irreducible representation (IR) of the lattice at $q=0$. (This IR is inferred from Raman experiments to be the B_{1g} representation.) To be consistent with the existence of a QCP, the lowered symmetry in region II must then be due to the condensation of such an operator. In the ordered state, the singularity in the Raman response must then disappear; this is also consistent with experiments in region II.[24]

An operator satisfying the above requirements is the *current* operator at $q=0$ in the B_{1g} representation of the lattice.[25,26] In a microscopic theory of the cuprates[4,5] based on a model suggested earlier,[27] it was predicted that the region II violates time-reversal symmetry by a ground state which carries currents in the O-Cu-O plaquettes in each cell. An experiment using ARPES with circularly polarized photons was suggested[28] to identify the T-breaking phase. Some detailed experiments have borne out these predictions.[11] New classes of experiments have been suggested to further verify the predicted phase.[29,30]

The violation of time-reversal symmetry is shown here to be accompanied by singular attractive forward scattering due to the generation of a retarded $1/q^2$ interaction. Due to such a scattering, the density of states of one-particle spectra at the chemical potential, projected to a particular IR of the lattice, tends to zero. The resulting stable state is shown to have an anisotropic gap in the single-particle spectra at the chemical potential.[5]

It is worthwhile summarizing the principal results observed in region II of the phase diagram. The principal property in this region is an anisotropic loss of low-energy excitations. First discovered in measurements of Knight shift,[21] this was soon found in the specific heat measurements,[22] as well as in direct measurements of the single-particle spectra through ARPES.[20] Transport properties, Raman scattering, and neutron scattering also show characteristic changes in their temperature (frequency) dependences below $T_p(x)$. This region is often said to have a *pseudogap*. This is a misnomer (which I am forced to persist in using). ARPES measurements show (see, for example, Figs. 26 and 28 of Ref. 31) that the anisotropic gap is as robust as the superconducting gap at a corresponding reduced temperature.

Contents of this paper. In this paper I focus on the broken symmetry as well as the generated anisotropic gap and the equilibrium properties and the single-particle spectra in region II. The density of states, the specific heat, and the magnetic susceptibility are calculated with remarkable correspondence with the experiments. The transport properties will be studied in the near future. The paper is organized as follows. The motivations for the specific model introduced for the cuprates are reiterated in Sec. II, where the physics of time-reversal violation or local circulating currents is related to the screening of charge fluctuations special to the cuprates. Time-reversal-violating (TRV) states are derived in mean-field calculations in Sec. III. A phase diagram similar to Fig. 1 is derived. The current patterns and the symmetries in this state are also discussed. In Sec. IV, the coupling functions of the collective fluctuations toward the TRV states of the fermions are derived to show why time-reversal violation must necessarily engender a Fermi-surface instability. The stable state is shown to have an anisotropic gap at the chemical potential. The single-particle spectrum and the thermodynamics are derived and compared with experiments and some predictions for further experiments may be found in Sec. VI.

An important result is that the derived coupling of the fluctuations in region I to the fermions suggests that the phenomenological spectrum of Eq. (1) should be modified in one respect: $\chi(\mathbf{q},\omega,T)$ should be replaced by $\chi(\mathbf{q},\mathbf{k},\omega,T)$ where at small momentum transfer $\mathbf{q}$, the $\mathbf{k}$ dependence near the Fermi surface varies with the dominant IR of the fluctuations.

Various sundry issues, including the limitations of the theory, are discussed in the concluding section.

II. THE MINIMAL MODEL FOR CUPRATES

A microscopic model for the cuprates must take into account that the phenomena observed in them hardly ever, if at all, occur in any other known compound. The effective Hamiltonian for the cuprates must therefore reflect some unique features of their solid-state chemistry. Consideration of this issue led to the three-orbital model with longer-range interactions as well as the local repulsions on Cu and on O.[27]

Cuprates have the unique feature that the ionization energy of the Cu^{2+} state is nearly equal to the affinity energy of the O^{2-} state, i.e., $E(Cu^{+})-E(Cu^{2+})$ is nearly equal to $E(O^{-})-E(O^{2-})$.[32] The corresponding difference is much larger than the one-particle transfer integrals in other transition metal oxides. Therefore the charge fluctuations in the metallic state occur almost equally on copper and on oxygen ions. The $4s$ and p orbitals on Cu are too far away in energy to screen the mixed-valence fluctuations on Cu intra-atomically; the $3s$ state of O are similarly too far away for intra-atomic screening. (These orbitals, when they control the screening, can be eliminated in favor of a renormalized effective repulsion parameter, the U of the Hubbard model.) Charge fluctuations can then only be screened by complementary charge fluctuations on the neighboring ions. A consequence is that the screening length is close to the nearest-neighbor Cu-O distance, giving large effective ionic interactions which summed over the nearest neighbors are of the same order as the local repulsion energies (U) on the Cu or O ions. Since both the ionization-affinity energy difference and the transfer integrals are smaller than the ionic interactions, there is no small parameter in the physics of the cuprates by which the ionic interactions may be absorbed to start with a simpler model such as the Hubbard and t-J model proposed[33] for the cuprates.

Whether the ionic interactions introduce qualitatively new properties can only be decided by calculations using them. I show in this paper that this is possible using approximate but systematic methods. For a range of ionic interactions and doping, screening can be achieved coherently through occupied wave functions which are complex admixtures of orthogonal orbitals in a unit cell, i.e., by currents in the elementary O-Cu-O plaquettes. Such coherent screening represents time-reversal violation.

The minimal model Hamiltonian[27] is on the basis of three orbitals per unit cell, d, p_x, p_y:

$$H = K + H_{int}^{(1)} + H_{int}^{(2)}. \tag{2}$$

K is the kinetic energy operator,

$$K = \sum_{\mathbf{k},\sigma} \epsilon_d n_{d\mathbf{k}\sigma} + 2t_{pd} d_{\mathbf{k},\sigma}^{\dagger}[s_x(k)p_{x\mathbf{k}\sigma} + s_y(k)p_{y\mathbf{k}\sigma}] - 4t_{pp}s_x(k)s_y(k)p_{x\mathbf{k}\sigma}^{\dagger}p_{y\mathbf{k}\sigma} + \text{H.c.} \tag{3}$$

Here a particular choice of the relative phases of the x and y orbitals in the unit cell has been made, $s_{x,y}(k) = \sin(k_x a/2, k_y a/2)$ and for later, $c_{x,y}(k) = \cos(k_x a/2, k_y a/2)$ and $s_{xy}^2(k) = \sin^2(k_x a/2) + \sin^2(k_y a/2)$. Note that $t_{pp} > 0$, irrespective of the choice of the relative phases of the orbitals. The local interactions on the Cu and the O orbitals are

$$H_{int}^{(1)} = \sum_{i,\sigma} U_d n_{di\sigma} n_{di\text{-}\sigma} + U_p(n_{pxi\sigma} n_{pxi\text{-}\sigma} + n_{pyi\sigma} n_{pyi\text{-}\sigma}) \tag{4}$$

and the nearest-neighbor interactions between the Cu and the O orbitals are

$$H_{int}^{(2)} = \sum_{i,\mathrm{NN}} V n_{di}(n_{i+\mathrm{NN},p_x} + n_{i+\mathrm{NN},p_y}), \tag{5}$$

where $(i+\mathrm{NN})$ stands for nearest O neighbors of Cu in a cell i with (p_x, p_y) orbitals in the (x,y) direction. In momentum space, this is

$$H_{int}^{(2)} = 2V \sum_{\mathbf{k}\mathbf{k}'\mathbf{q},\sigma\sigma'} c_x(q) d_{\mathbf{k}+\mathbf{q}\sigma}^{\dagger} d_{\mathbf{k}\sigma} p_{x\mathbf{k}-\mathbf{q}\sigma'}^{\dagger} p_{x\mathbf{k}'\sigma'} + x \to y. \tag{6}$$

We may also include the nearest-neighbor interactions between the O orbitals or longer-range interactions. Such interactions do not change the essential results derived here provided they are small compared to V. In the calculations in this paper the (renormalized) energy difference ϵ_d between the Cu and the O orbitals is taken as zero. It is important that in CuO, $\epsilon_d \lesssim O(t_{pd})$. Taking it as zero simplifies the calculations presented; the principal effect of a finite ϵ_d will be mentioned.

In the limit that $(U_d, U_p) \gg (t_{pd}, t_{pp})$, a good approximation[34] for small deviations $|x|$ from half filling consists in replacing[34]

$$t_{pd} \to \bar{t}_{pd} = t_{pd}|x|, \quad t_{pp} \to \bar{t}_{pp} = t_{pp}|x|, \tag{7}$$

where $|x|$ is the deviation from half filling; $x > 0$ for holes and $x < 0$ for electrons. The Lagrange parameter appropriate to this transformation is absorbed in the chemical potential. A more general and messy mean-field calculation would consider separately the average occupations in the oxygen and copper orbitals and renormalize t_{pd}, t_{pp} accordingly. It is not expected to change any of the essential results.

An alternate treatment[4] to handle the large local and ionic repulsions is to start from the strong-coupling limit by diagonalizing a unit cell exactly[35,36] by cutting of its kinetic energy connection to its neighbors and then to introduce the kinetic energy connecting the lowest-energy many-body states in each cell. This is a generalization of the procedure by which the t-J Hamiltonian is derived from the Hubbard model. Starting from the model of Eq. (1), this leads minimally to an effective $\mathrm{SU}(2) \times \mathrm{SU}(2)$ Hamiltonian plus the constrained kinetic energy; one SU(2) represents the usual spin space while the other represents the two lowest many-body states obtained in each cell by the first step in the procedure,

$$H_{int} = \mathcal{J}(-1/2 + \sigma_i \cdot \sigma_j)(\mathbf{A} + \tau_i \mathbf{B} \tau_j). \quad (8)$$

Here the τ's are in the orbital space and $\mathbf{A}, \mathbf{B}$ give the anisotropy of interactions in that space. This Hamiltonian leads to solutions with the same symmetries as in the approach below.

III. DERIVATION OF TIME-REVERSAL-VIOLATING STATES

Time-reversal-violating states are shown here in a mean-field approximation to be possible stable states for the model in a range of parameters. To construct a mean-field theory, write the interactions of Eq. (5) in a separable form,

$$H_{int}^{(2)} = -V \sum_{i=1,\ldots,4,\mathbf{k},\mathbf{q},\sigma} A_{\mathbf{q},\mathbf{k},\sigma}^{\dagger(i)} \sum_{\mathbf{k}',\sigma'} A_{\mathbf{k}',\mathbf{q},\sigma'}^{(i)}, \quad (9)$$

$$A_{\mathbf{k},\mathbf{q},\sigma}^{(1,2)} = s_x(\mathbf{k}) p_{x,\mathbf{k}+\mathbf{q},\sigma}^{\dagger} d_{\mathbf{k},\sigma} \pm s_y(\mathbf{k}) p_{y,\mathbf{k}+\mathbf{q},\sigma}^{\dagger} d_{\mathbf{k},\sigma}, \quad (10)$$

$$A_{\mathbf{k},\mathbf{q},\sigma}^{(3,4)} = c_x(\mathbf{k}) p_{x,\mathbf{k}+\mathbf{q},\sigma}^{\dagger} d_{\mathbf{k},\sigma} \pm c_y(\mathbf{k}) p_{y,\mathbf{k}+\mathbf{q},\sigma}^{\dagger} d_{\mathbf{k},\sigma}. \quad (11)$$

The superscripts (1,3) and (2,4) refer to the plus and minus signs, respectively.

A model such as that in Eq. (2) is a severe simplification of the problem. It may be the minimum essential model but the parameters that faithfully represent the actual problem through it are knowable to factors of 2 at best. Staggered flux phases,[37,38] charge-density waves,[39] spin-density waves, charge-transfer instabilities,[40,41] etc. may be produced in mean field by the same Hamiltonian by varying different parameters. It is not the purpose of this paper to find the phase diagram for all these instabilities in the space of the parameters of the Hamiltonian, but to show that the trial states chosen for investigation by discarding those that can be excluded on the basis of experiments occur for reasonable physical parameters, and let experiments decide whether they indeed occur.

Accordingly, I choose to look only for mean-field solutions that do not break translational symmetry and/or spin-rotational symmetry. For such solutions, one needs to consider only the zero-momentum transfer, $q=0$, part of the Hamiltonian $H_{int}^{(2)}$. We can therefore introduce a possible mean-field order parameters $R_i \exp(i\phi_i)$ and rewrite

$$H_{int}^{(2)} = -V \sum_{\mathbf{q},i} \left(\sum_{\mathbf{k},\sigma} A_{\mathbf{k},\mathbf{q},\sigma}^{(i)\dagger} - \delta_{\mathbf{q},0} R_i/V \exp(-i\phi_i) \right) \times \left(\sum_{\mathbf{k}',\sigma} A_{\mathbf{k}',\mathbf{q},\sigma}^{(i)} - \delta_{\mathbf{q},0} R_i/V \exp(i\phi_i) \right) + \sum_i R_i^2/V - R_i \sum_{\mathbf{k},\sigma} [A_{\mathbf{k},0,\sigma}^{(i)} \exp(i\phi_i) + A_{\mathbf{k},\mathbf{0},\sigma}^{(i)\dagger} \exp(-i\phi_i)],$$

$$R_i \exp(i\phi_i) = V \sum_{\mathbf{k},\sigma}{}' \langle A_{\mathbf{k},0,\sigma}^{(i)} \rangle. \quad (12)$$

The sum over $\mathbf{k}$ in R's is restricted to the occupied part and the expectation value is in the state to be determined self-consistently.

The mean-field Hamiltonian with order parameter at $\mathbf{q}=\mathbf{0}$ can only be a 3×3 matrix in the space of the three orbitals per unit cell at each $\mathbf{k}$. Furthermore, the effective single-particle energy for the p_x and p_y orbitals must be kept degenerate; the renormalization of their difference from the energy of the d orbital can produce a charge-transfer instability[41] which is generically of first order and therefore not of interest. (We will take the point of view that such renormalizations have already been taken into account in the bare parameters of the theory.) This leaves only three functions of $\mathbf{k}$ in the off diagonals to be determined. The $q=0$ part of $A^{(1)}$ transforms simply as the existing kinetic energy and cannot lead to a broken symmetry. If a real order parameter is constructed from the rest of $H_{int}^{(2)}$, a structural distortion of the unit cell is a necessary accompaniment. We discard this possibility as well. So the order parameter must be nonreal. As will be obvious below, $A^{(3)}$ and $A^{(4)}$ lead to different domains of the same phase. So a mean-field theory of $H_{int}^{(2)}$ of Eq. (5), not in conflict with experiments, can produce only two distinct order parameters:

$$R_I \exp(i\phi_I) = V \sum_{\mathbf{k},\sigma}{}' \langle A_{\mathbf{k},0,\sigma}^{(2)} \rangle = \pm V \sum_{\mathbf{k},\sigma}{}' [s_x \langle p_{x\mathbf{k},\sigma}^{\dagger} d_{\mathbf{k},\sigma} \rangle - s_y \langle p_{y,\mathbf{k},\sigma}^{\dagger} d_{\mathbf{k}} \rangle], \quad (13)$$

$$R_{II} \exp(i\phi_{II}) = V \sum_{\mathbf{k},\sigma}{}' \langle A_{\mathbf{k},0,\sigma}^{(3,4)} \rangle = \pm V \sum_{\mathbf{k},\sigma}{}' [c_x \langle p_{x\mathbf{k},\sigma}^{\dagger} d_{\mathbf{k},\sigma} \rangle \pm c_y \langle p_{y,\mathbf{k},\sigma}^{\dagger} d_{\mathbf{k},\sigma} \rangle]. \quad (14)$$

In the mean-field approximation the expectation value of the constrained kinetic energy plus $H_{int}^{(2)}$ is minimized to determine the order parameter R. For the state Θ_I, the mean-field Hamiltonian is

$$\mathcal{H}_{MF}^{I} = K + R_I^2/V - R_1 \exp(-i\phi_I) \times \sum_{\mathbf{k},\sigma} [s_x(\mathbf{k}) p_{x\mathbf{k},\sigma}^{\dagger} d_{\mathbf{k},\sigma} - s_y(\mathbf{k}) p_{y\mathbf{k},\sigma}^{\dagger} d_{\mathbf{k},\sigma}] + \text{H.c.} \quad (15)$$

For the state Θ_{II}, the mean-field Hamiltonian is

$$\mathcal{H}_{MF}^{II} = K + R_{II}^2/V - R_{II} \exp(-i\phi_{II}) \times \sum_{\mathbf{k},\sigma} [c_x(\mathbf{k}) p_{x\mathbf{k},\sigma}^{\dagger} d_{\mathbf{k},\sigma} - c_y(\mathbf{k}) p_{y\mathbf{k},\sigma}^{\dagger} d_{\mathbf{k},\sigma}] + \text{H.c.} \quad (16)$$

For both states the first and the third terms of the *mean-field* Hamiltonian written in the space of the orbitals $d_{\mathbf{k}}, p_{x\mathbf{k}}, p_{y\mathbf{k}}$ is the matrix

$$\mathcal{H}_{MF}=\begin{pmatrix} 0 & 2\bar{t}_{pd}e^{i\theta_x(\mathbf{k})}|s_x(\mathbf{k})| & 2\bar{t}_{pd}e^{i\theta_y(\mathbf{k})}|s_y(\mathbf{k})| \\ 2\bar{t}_{pd}e^{-i\theta_x(\mathbf{k})}|s_x(\mathbf{k})| & 0 & -4\bar{t}_{pp}s_x(\mathbf{k})s_y(\mathbf{k}) \\ 2\bar{t}_{pd}e^{-i\theta_y(\mathbf{k})}|s_y(\mathbf{k})| & -4\bar{t}_{pp}s_x(\mathbf{k})s_y(\mathbf{k}) & 0 \end{pmatrix}. \tag{17}$$

For the state Θ_I

$$\tan\theta_x=\frac{R_I\sin\phi_I}{2t_{pd}+R_I\cos\phi_I},\quad \tan\theta_y=\frac{-R_I\sin\phi_I}{2t_{pd}-R_I\cos\phi_I}, \tag{18}$$

while for the state Θ_{II}

$$\tan[\theta_x(k)]=\frac{R_{II}c_x\sin\phi_{II}}{2\bar{t}_{pd}s_x+R_{II}c_x\cos\phi_{II}},\quad \tan[\theta_y(k)]=\pm\frac{R_{II}c_y\sin\phi_{II}}{2\bar{t}_{pd}s_y\pm R_{II}c_y\cos\phi_{II}}. \tag{19}$$

The unitary (gauge) transformation

$$d_{\mathbf{k},\sigma}\to d_{\mathbf{k},\sigma},\quad p_{x,\mathbf{k},\sigma}\to p_{x,\mathbf{k},\sigma}\exp(i\theta_x),\quad p_{y,\mathbf{k},\sigma}\to p_{y,\mathbf{k},\sigma}\exp(i\theta_y)$$

on Eq. (17) transforms it to

$$\begin{pmatrix} 0 & 2\bar{t}_{pd}|s_x(\mathbf{k})| & 2\bar{t}_{pd}|s_y(\mathbf{k})| \\ 2\bar{t}_{pd}|s_x(\mathbf{k})| & 0 & -4\bar{t}_{pp}e^{i(\theta_x-\theta_y)}s_x(\mathbf{k})s_y(\mathbf{k}) \\ 2\bar{t}_{pd}|s_y(\mathbf{k})| & -4\bar{t}_{pp}e^{i(\theta_y-\theta_x)}s_x(\mathbf{k})s_y(\mathbf{k}) & 0 \end{pmatrix}. \tag{20}$$

Note that

$$\theta(\mathbf{k})\equiv\theta_x(\mathbf{k})-\theta_y(\mathbf{k}) \tag{21}$$

is the invariant *flux* associated with the elementary O-Cu-O plaquette. [The correspondence of the theory here to the generation of time-reversal violation in the SU(3) model of elementary particles through the Cabibbo-Kobayashi-Masakawa SU(3) mass matrix[42] may be noted. The time-reversal violation there is in an abstract space; here the phenomenon is more vividly pictured.] The problem therefore reduces to determining this invariant by minimization of the free energy.

Returning to the minimization, since at any $\mathbf{k}$ the trace over the three bands is conserved, the change in ground-state energy can be calculated from the change in energy of the unfilled part of the conduction band alone. In the Appendix these are calculated to leading order in t_{pp}/t_{pd}. The value of the phase $\phi_{I,II}$ at the minimum is found to be at

$$\phi=\pm\pi/2. \tag{22}$$

With $\epsilon_d=0$ and the deviation from half filling $|x|\ll 1$, $\theta_{1,2}\neq 0$ at $T=0$ only if

$$V\gtrsim 2a_{1,2}\frac{|x|}{(1+x)}t_{pd}^2/t_{pp}, \tag{23}$$

where $a_{1,2}$ are numerical coefficients of order unity, which depend on the details of the band structure and whether the state is Θ_I or Θ_{II}. The equality in Eq. (23) provides the hole ($x_c>0$) and the electron ($x_c<0$) densities at the QCP's. In the Appendix it is shown that the simplest model favors the Θ_{II} phase. Only the possibility of the Θ_I phase was considered earlier.[5] Equation (23) gives that for $V\simeq t_{pd}\simeq 2t_{pp}$, $x_c\simeq 0.1$ which, in view of the approximations made, is surely a stroke of luck.

In the Appendix the transition temperature is also derived to find

$$T_g\propto E_f/\ln(1-x/x_c),\quad x\leqslant x_c, \tag{24}$$

where E_f is the Fermi energy in the conduction band. At $x\to 0$, this result is an artifact of the model with ϵ_d taken zero. (At $x\to 0$, the effective masses in all bands are infinite, so that for $\epsilon_d=0$ the bands are degenerate and the transition occurs for $V\to 0$ at $T\to 0$ or infinite T at V finite.) Moreover competition of antiferomagnetism and the TRV state has not been considered here. The result is therefore only valid for x close to $x_c\ll 1$. Equations (23) and (24) give the correct general shape for the phase II marked in Fig. 1 for x below and near x_c.

The mean-field wave function is made up of products of $|\mathbf{k},\theta_1\sigma\rangle$ up to the Fermi vector. In the original gauge, i.e., in which Eqs. (2) and (15) are written, the new (TRV) conduction band wave functions for either state Θ_I or Θ_{II} to leading order in t_{pp}/t_{pd} are (the spin index is suppressed)

$$c^\dagger_{\mathbf{k},\theta_1}|0\rangle=(N_k)^{-1}\Bigg(a^\dagger_{\mathbf{k}}+2\frac{\bar{t}_{pp}s_xs_y}{\epsilon^0_{\mathbf{k}}s^2_{xy}}\{(s_x^2-s_y^2)\cos[\theta_{(1,2)}(\mathbf{k})]+is^2_{xy}\sin[\theta_{(1,2)}(\mathbf{k})]n^+_{\mathbf{k}}\}\Bigg)|0\rangle,$$

$$a^+_{\mathbf{k}}=\frac{d^\dagger_k}{\sqrt{2}}+\left(\frac{s_xp^\dagger_{kx}\exp(-i\theta_x)+s_yp^\dagger_{ky}\exp(-i\theta_y)}{\sqrt{2}s_{xy}}\right),$$

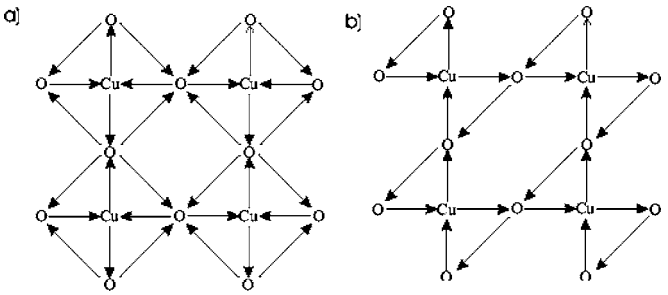

FIG. 2. The current pattern in the time-reversal-violating state (a) Θ_I and (b) Θ_{II}.

$$n_{\mathbf{k}}^{+} = [s_y p_{kx}^{\dagger} \exp(-i\theta_x) - s_x p_{ky}^{\dagger} \exp(-i\theta_y)]/s_{xy}. \quad (25)$$

$\epsilon_{\mathbf{k}}^{0} = 2\bar{t}_{pd} s_{xy}(\mathbf{k})$ and N_k are normalization factors. $\theta_1(\mathbf{k})$ are variationally determined:

$$\theta_1(\mathbf{k}) = \pm \langle R_I \rangle / 2\bar{t}_{pd} \quad \text{for state } \Theta_I,$$

$$\theta_2(\mathbf{k}) = \pm (\langle R_{II} \rangle / 2\bar{t}_{pd})[\cot(\mathbf{k}_x a) \pm \cot(\mathbf{k}_y a)] \quad \text{for state } \Theta_{II}. \quad (26)$$

These expressions are obtained from Eqs. (18) and (19) for $\langle R \rangle / \bar{t}_{pd} \ll 1$ and k_x, k_y not close to zero for Θ_{II}.

A. Symmetries of the mean-field TRV Hamiltonian

It is useful to recall that a complex Hamiltonian that cannot be transformed to a real operator by any unitary (gauge) transformation does not commute with the time-reversal operator $\mathcal{R}$ and therefore has eigenstates which break time-reversal invariance. Correspondingly, its eigenstates cannot be transformed to be real by any unitary transformation. This is true of the wave functions of Eqs. (25) and (26). So time reversal is violated in the phases found. Further, if

$$H(\theta)|k, \theta, \sigma\rangle = \epsilon(\mathbf{k}, \theta)|\mathbf{k}, \theta, \sigma\rangle \quad (27)$$

$\mathcal{R}|\mathbf{k}, \theta, \sigma\rangle$ is not an eigenstate of $H(\theta)$ but is of $\mathcal{R}^{-1} H(\theta) \mathcal{R}$ with the same eigenvalue $\epsilon(\mathbf{k}, \theta)$.

Consider the state Θ_I. Physically, $\theta_1/2$ and $-\theta_1/2$ are the phase differences between the d orbital and the p_x and p_y orbitals, respectively, in each unit cell. The total phase difference θ_1 in going around any of the four triangular plaquettes in each unit cell is gauge invariant and can be distributed between the three legs of the plaquettes in any way one chooses by an appropriate gauge transformation. If we include additional interactions which produce additional phase shifts between the vertices of the plaquettes (for example a repulsion between electrons on the neighboring oxygen orbitals produces in a mean-field approximation a phase shift between the p_x and the p_y orbitals of each unit cell) it can be absorbed in the invariant flux. A finite flux in a plaquette is equivalent to a current circulating around the plaquette. The current pattern for (one of the two domains of) the state Θ_I is shown in Fig. 2. This current pattern can be found by transforming the wave functions to real space and calculating the expectation value of the current operator between the sites of the lattice. The magnitude of the current is of $O(\theta_1 t_{pp} \bar{t}_{pd}^2 a^3)$.

The symmetry of the current pattern follows from the properties upon applying the reflection operator $\sigma_{\hat{m}}$ about a mirror plane $\hat{m}$ on the wave functions (25) and (26). When $\hat{m}$ is the $x=0$ or the $y=0$ plane, the wave functions are eigenstates of $\sigma_{\hat{m}}$. But reflection symmetry is broken about the *crystalline* mirror planes $x=\pm y$. Note that if we consider properties that depend on the modulus of the wave functions, for example, the charge density, mirror plane symmetries existing for $\theta=0$ are preserved for $\theta \neq 0$. A current-sensitive experiment (sensitive linearly to the wave function and its gradient) can therefore detect a time-reversal-breaking phase through the difference in reflection symmetries, but experiments sensitive only to charge distributions cannot.

It may also be seen from the wave functions that fourfold rotation (C_4) about an axis through the Cu's is not a symmetry but the rotation followed by time-reversal $C_4\mathcal{R}$ is a symmetry. Also the center of inversion is preserved. The simplest *lattice* symmetry for the Cu-O compounds is $4/mmm$; the lowered symmetry generated below the transition is $4/\underline{m}mm$ in the double-group notation.[43]

In the state Θ_{II}, reflection symmetry is lost about the *crystalline* mirror planes $x=0$ and $y=0$. The states with plus signs between the p_x and the p_y parts in the expression for θ_2 keep reflection symmetry about $x=y$ mirror planes but not about the $x=-y$ mirror planes; the converse is true for the state with the minus sign. The current pattern for the former is also shown in Fig. 2. Inversion is lost in this phase but the product of inversion and time reversal is preserved. Such phases are called *magnetoelectric*.[44] Starting from a lattice of symmetry $4/mmm$, the reduced new symmetry is $m\underline{m}m$. These issues are further discussed in Ref. 29, where extensions to more complicated lattice structures are also given. Note that the Θ_{II} phase has four domains.

One may check[43] that neither the Θ_I, i.e., $4/\underline{m}mm$, nor the Θ_{II} phase, i.e., the $m\underline{m}m$, is *piezomagnetic*; the application of a uniform magnetic field does not linearly change the symmetry of the unit cell.

The polarized ARPES experiments[11] are consistent with the state Θ_{II} in region II of the phase diagram in Fig. 1.[45] It follows that if the superconducting transition is a continuous transition, the symmetry breaking of the pseudogap state, both time reversal and inversion, should continue in the superconducting region[30,46] to the left of the QCP in Fig. 1. An experimental evidence for this would constitute a further direct test of the theory of the cuprates presented here.

The interesting property that chiral spin correlations accompany orbital currents of fermions ought to be mentioned.[47] For three sites (i,j,k), and current operators J_{ij} from site i to site j, etc., the expectation value

$$\langle J_{ij} J_{jk} J_{ki} \rangle \propto \langle \mathbf{s}_i \cdot (\mathbf{s}_j \times \mathbf{s}_k) \rangle, \quad (28)$$

where $\mathbf{s}_i$ is the spin operator at the site i. [The order parameter θ is proportional to this current expectation value with (i,j,k) forming the nearest-neighbor O-Cu-O triangular plaquettes.] Therefore chiral spin order always accompanies the orbital current order.

IV. THE FERMI-SURFACE INSTABILITY OF THE TRV STATES

The TRV instability derived above is due to the mixing of states from different bands (equivalently due to mixing of different-correlated orbitals in a unit cell if we start from the strong-coupling end) due to large enough screening interactions. It is not a Fermi-surface instability and by itself does not create a gap at the chemical potential. I show here that such a TRV state cannot exist with a normal Fermi surface. The stable state has an anisotropic gap at the chemical potential. TRV as well as translational symmetry is preserved in the new state.

Consider the *classical* fluctuation regime in the transition to the TRV-breaking phase. (This should be distinguished from the regime I of the phase diagram in Fig. 1.) The simplest representation of the current fluctuations in this regime has a propagator of the form

$$\chi_c(\mathbf{q},\omega) \propto (i\omega/\gamma_0 + \kappa^2|q|^2 + \epsilon)^{-1}. \tag{29}$$

ϵ is the distance to the transition $|T_g - T|/T_g$ but the region close to the QCP at $T_g = 0$ is excluded from the considerations here. Since the fluctuations are of an unconserved quantity, the leading term in their damping is a constant denoted here by γ_0. The dynamics belongs to model A in the classification of Halperin and Hohenberg.[48] Since the order parameter is also a discrete variable, the fluctuations have a finite coupling to the fermions in the long-wavelength limit. This is shown explicitly below. Due to the infinite range of the fluctuations, the normal Fermi surface cannot be stable. This is seen in a calculation of the fermion self-energy due to exchange of the fluctuations of Eq. (29). One finds that for $|\mathbf{k}-\mathbf{k}_f| \to 0$,

$$\Sigma(\mathbf{k},\nu) = |\gamma(\hat{k}_f)|^2 \sum_{\mathbf{q}} \int_{-\infty}^{\infty} d\omega \frac{\mathrm{Im}\,\chi_c(\mathbf{q},\omega)}{\nu + \omega - \epsilon_{\mathbf{k}+\mathbf{q}} + i\delta} \times [\coth(\omega/2T) + \tanh(\epsilon_{\mathbf{k}+\mathbf{q}}/2T)]. \tag{30}$$

$g(\hat{k}_f)$ is the coupling function of the fermions to the long-wavelength fluctuations, derived below. For a classical transition, we may take $\omega \ll T$ and consider the pole in χ_c to be much more important than the denominator in Eq. (30). Then on removing ω from the denominator and noting that the integral of Im χ_c over ω is 0, one is left to evaluate only

$$\Sigma(\mathbf{k},\nu) \approx 2T|\gamma(\hat{k}_f)|^2 \sum_{\mathbf{q}} \frac{1}{\nu - \epsilon_{\mathbf{k}+\mathbf{q}} + i\delta} \int_{-T}^{T} d\omega \frac{1}{\omega^2 + (a^2q^2 + \epsilon)^2}. \tag{31}$$

This gives for small ν and small $\mathbf{k}-\mathbf{k}_f$ that

$$\Sigma(\mathbf{k},\nu) \propto \begin{cases} |\gamma(\hat{k}_f)|^2 (\nu + |\mathbf{k}-\mathbf{k}_f| + \epsilon)^{-1} \ln(\nu + |\mathbf{k}-\mathbf{k}_f| + \epsilon) & \text{in two dimensions,} \quad (32) \\ |\gamma(\hat{k}_f)|^2 \ln(\nu + |\mathbf{k}-\mathbf{k}_f| + \epsilon) & \text{in three dimensions.} \quad (33) \end{cases}$$

Recall that the self-energy due to (unscreened) Coulomb interactions in the Hartree-Fock approximation has a $\ln|\mathbf{k}-\mathbf{k}_f|$ divergence in three dimensions (3D) and a $|\mathbf{k}-\mathbf{k}_f|^{-1}$ divergence in 2D. Here because of the retarded nature of the effective Coulomb interaction, the singularities in $|\mathbf{k}-\mathbf{k}_f|$ and ν are identical. The Hartree-Fock singularities are eliminated when screened interactions are considered. In the present problem, such singularities are protected in the vicinity of the TRV transition.

The renormalized Fermi velocity is given by

$$\mathbf{v}(\mathbf{k}_f)/\mathbf{v}_{f0} = z(1 + \mathbf{v}_{f0}^{-1} \cdot \partial\Sigma/\partial\mathbf{q})\big|_{\mathbf{k}_f,\mu}, \tag{34}$$

where $\mathbf{v}_{f0}$ is the bare Fermi velocity and z is the quasiparticle renormalization, $z = (1 + \partial\Sigma/\partial\omega)^{-1}|_{\mathbf{k}_f,\mu}$. Therefore the Fermi velocity is not renormalized due to the cancellation in the divergence in the frequency and momentum dependence of the self-energy. However, the quasiparticle density of states at the Fermi surface is given by

$$N(\hat{k}_f)/N_0 = (1 + \mathbf{v}_{f0}^{-1} \cdot \partial\Sigma/\partial\mathbf{q})^{-1}\big|_{\mathbf{k}_f,\mu}. \tag{35}$$

Therefore the partial density of states at the Fermi surface in the irreducible representation of $|\gamma(\hat{k}_f)|^2$ tends to 0 as $\epsilon \to 0$. If the partial density of states in any IR approaches 0, a compressibility in that IR approaches 0, signifying an instability. The cure to this instability is shown through an explicit calculation below to be a state with a gap in the density of states in the IR in which $g(\hat{k}_f)$ is maximum. The connection of this situation to the Landau-Pomeranchuk instabilities is discussed in Ref. 49. Since the instability necessarily accompanies the classical fluctuation regime of the TRV transition, the two must occur together, as is also shown below.

A. Coupling of the fluctuations to the fermions

In this section the coupling functions $\gamma(\mathbf{k})$ are derived in the fluctuation regime of the TRV state and the TRV state itself. To this end, the mean-field Hamiltonian Eqs. (15) and (16) is supplemented by the terms giving the fluctuations in Eq. (12).

In the Θ_I phase, the fluctuations either change the magnitude of the order parameter ($\theta_1 \to \theta_1 + \delta\theta_{\mathbf{q}}$) or admix the states of the *other* domain ($\phi \to \pm\pi/2 + \delta\phi_{\mathbf{q}}$). The last two terms of Eq. (12) have been used in H_{MF}. The first term is used to generate the fluctuations. To this end, one writes

$$\sum_{\mathbf{k},\mathbf{q}} A_{\mathbf{k},\mathbf{q}} = (\theta_1 + \delta\Phi_{\mathbf{q}}/V)\exp[i(\phi_0 + \delta\phi_{\mathbf{q}})] + \text{incoherent part}. \tag{36}$$

The incoherent part is the fermionic part of the fluctuations which is expressed in terms of the new particle-hole states in the Θ phases. The coherent part are the bosonic fluctuations. In the fluctuation regime to the Θ states, $\theta=0$, and the only fluctuations are the amplitude fluctuations $\delta\theta_{\mathbf{q}}$ in the simple small-fluctuation approximation used here.

The fermion-boson coupling Hamiltonian follows directly by finding the matrix elements of the fermionic part of $A_{\mathbf{k},\mathbf{q}}$ in the wave functions given in Eqs. (25) and (26). The results are

$$H_{FB} = \sum_{\mathbf{k},\mathbf{k}'} c^{\dagger}_{\mathbf{k}',\theta} c_{\mathbf{k},\theta} [\gamma_p(\mathbf{k},\mathbf{k}')(\delta\theta_{(\mathbf{k}-\mathbf{k}')} + \delta\phi^{\dagger}_{-(\mathbf{k}-\mathbf{k}')}) + \gamma_a(\mathbf{k},\mathbf{k}')(\delta\theta_{(\mathbf{k}-\mathbf{k}')} + \delta\theta^{\dagger}_{-(\mathbf{k}-\mathbf{k}')})]. \tag{37}$$

In the next section we will be interested in the coupling only in the forward scattering limit ($\mathbf{k}-\mathbf{k}' \to 0$). In this limit, for the Θ_1 phase,

$$\gamma_a(\mathbf{k},\mathbf{k}) \approx V\theta_1[1 + \cos(k_x a) + \cos(k_y a)],$$

$$\gamma_p(\mathbf{k},\mathbf{k}) \approx V\theta_1[\cos(k_x a) - \cos(k_y a)]. \tag{38}$$

The energy of the phase mode at long wavelengths is calculated in the Appendix to be

$$\Omega_{\phi} \approx \frac{\bar{t}_{pp}^2}{\bar{t}_{pd}}\theta_1^2. \tag{39}$$

The energy of the amplitude mode can be shown to be higher by a numerical factor of $O(2)$.

In the fluctuation regime, the only coupling is to the amplitude mode. The leading forward scattering coupling has the dependence,

$$\gamma_{fluct}(\mathbf{k},\mathbf{k}) \approx (V/2)[\cos(k_x a) - \cos(k_y a)]. \tag{40}$$

In the Θ_{II} phase the fluctuations may change the magnitude of the order parameter ($\theta_2 \to \theta_2 + \delta\theta_{\mathbf{q}}$), admix the states of the *other* time-reversed phase $\phi \to \pm\pi/2 + \delta\phi_{\mathbf{q}}$, or admix the states of the other *spatial* domain, i.e., admix states with reflection symmetry about $(\hat{x}+\hat{y})$ if the mean-field state chosen is the one with reflection symmetry about $(\hat{x}-\hat{y})$, or vice versa. We will call the operator for the last $\delta\theta_{m,\mathbf{q}}$. So in addition to the two kinds of coupling in Eq. (37), a coupling to fluctuations $\delta\theta_{m,\mathbf{q}} + \delta\theta^{\dagger}_{m,\mathbf{q}}$ with a coupling function $\gamma_m(\mathbf{k}+\mathbf{q},\mathbf{k})$ must be included.

To ensure a gauge-invariant calculation in the Θ_{II} phase, a Hamiltonian with a larger symmetry than that used to generate the mean-field state must be used. A minimum such Hamiltonian includes both the $A_3^{\dagger}A_3$ and $A_4^{\dagger}A_4$ terms of Eq. (9). We can then follow the familiar procedure to generate the coupling functions in the forward scattering limit for the three modes already described: For the amplitude mode, phase mode, and the "mixing mode" we get, respectively,

$$\gamma_a(\mathbf{k},\mathbf{k}) \approx V\theta_2[\cos(k_x a) + \cos(k_y a)], \tag{41}$$

$$\gamma_p(\mathbf{k},\mathbf{k}) \approx V\theta_2[\sin(k_x a) \pm \sin(k_y a)], \tag{42}$$

$$\gamma_m(\mathbf{k},\mathbf{k}) \approx V\theta_2[\cos(k_x a) - \cos(k_y a)]. \tag{43}$$

The energy of these modes in the long-wavelength limit is estimated in the Appendix. The energy of the phase mode Ω_{ϕ} is about the same as that in the phase Θ_I. The energy of the mixing mode at long wavelengths Ω_m is estimated in the Appendix to be about 1/2 of these. Therefore the important mode to consider for stability in the state Θ_{II} is the mixing mode.

The forward scattering with the amplitude fluctuations in the fluctuation regime has a dependence

$$\gamma_{fluct}(\mathbf{k},\mathbf{k}) \approx (V/2)[\sin(k_x a) \pm \sin(k_y a)]. \tag{44}$$

I have only considered small fluctuations in the above. The model also has interesting topological fluctuations (mentioned in the concluding section).

B. Anisotropic gap (pseudogap) in the TRV state

In the first part of this section, I presented an argument from $T \gtrsim T_g$ that the TRV phase has a tendency to develop an anisotropic gap at $T=T_g$. Now, I present a calculation coming to the same conclusion from $T \lesssim T_g$. In effect, the zero-order collective modes in the TRV phase, whose frequencies are estimated above, are shown to be unstable due to renormalizations by H_{FB} with a normal Fermi surface.

The effective Hamiltonian in the TRV phase is

$$H^{trv}_{eff} = \sum_{\mathbf{k}\sigma} \epsilon(\mathbf{k},\sigma) c^{\dagger}_{\mathbf{k},\sigma} c_{\mathbf{k},\sigma} + \sum_{\mathbf{q}} \Omega(\mathbf{q}) b^{\dagger}(\mathbf{q}) b(\mathbf{q}) + H_{FB}. \tag{45}$$

H_{FB} is given by Eq. (37). The annihilation and creation operators of the fluctuation modes are denoted by b and $b^{\dagger}$. The fluctuations with the lowest energies are of interest. They are the fluctuations of the phase for the Θ_I phase and the mixing fluctuations for the Θ_{II} phase. The operators $b(\mathbf{q}), b^{\dagger}(\mathbf{q})$ will only refer to these. We may eliminate these fluctuations and H_{FB} to generate a retarded effective interaction between the fermions of the form

$$\sum_{\mathbf{k},\mathbf{k}',\mathbf{q},\sigma,\sigma'} \gamma(\mathbf{k},\mathbf{k}+\mathbf{q})\gamma(\mathbf{k}'-\mathbf{q},\mathbf{k}') \times \chi_c(q,\omega) c^{\dagger}_{\mathbf{k}+\mathbf{q}\sigma} c_{\mathbf{k}\sigma} c^{\dagger}_{\mathbf{k}'-\mathbf{q}\sigma'} c_{\mathbf{k}'\sigma'}, \tag{46}$$

where $\chi_c(q,\omega)$ is the propagator for the relevant fluctuations. χ_c may be approximated by $-2/\Omega_q^0$ with a cutoff such that $\epsilon(k')$, $\epsilon(k'+q)$ are both within about ω_c of the chemical potential. The effective interaction is repulsive for states at higher energies. We use only the forward scattering part of the interactions, i.e., in the limit of small $\mathbf{q}$, and for $\mathbf{k},\mathbf{k}'$ close to the Fermi surface,

$$g(\mathbf{k},\mathbf{k}') = -\lim_{\mathbf{q}\to 0} 2\gamma(\mathbf{k},\mathbf{k}+\mathbf{q})\gamma(\mathbf{k}'-\mathbf{q},\mathbf{k}')/\Omega_{\mathbf{q}}, \tag{47}$$

with a cutoff of order $\omega_c \approx \Omega_0$. If $\Omega_0 \to 0$, the cutoff ω_c is approximately the larger of Ω_0 or the damping of the collective mode $\gamma_0|\epsilon$ of Eq. (29).

The instability seen through Eq. (30) may also be seen through the equation of motion for the *fluctuations* $\langle c^{\dagger}_{\mathbf{k+q},\sigma} c_{\mathbf{k},\sigma}\rangle$. Just as for Landau-Pomeranchuk instabilities, no solution for such equations can be found for real frequencies in the limit of small $\mathbf{q}$.[49,50] The cure to this instability is a new state in which particles are annihilated and created by operators $\tilde{c}^{\dagger}_{\mathbf{k},\sigma}, \tilde{c}_{\mathbf{k},\sigma}$, respectively, such that a stable homogeneous equation for

$$\langle \tilde{c}^{\dagger}_{\mathbf{k+q},\sigma'} \tilde{c}_{\mathbf{k},\sigma}\rangle(\mathbf{q},\nu) \tag{48}$$

at $\nu=0$ can be found at $\mathbf{q}$. Correspondingly, in the stable state, the one-particle eigenvalues are renormalized from $\epsilon_{\mathbf{k}\theta\sigma}$ to $E_{\mathbf{k}\sigma}$. Actually, the interactions $\gamma(\mathbf{k},\mathbf{k}')$ are renormalized also. But such strong-coupling corrections are not considered here. The particular form for $E_{\mathbf{k}\sigma}$ and the relation of the $\tilde{c}$'s to c's, etc., is dictated by the self-consistency condition derived below.

A stable state is chosen in which $\langle c^{\dagger}_{\mathbf{k+q},\sigma} c_{\mathbf{k},\sigma}\rangle$, and $\langle b_{\mathbf{q}}\rangle, \langle b^{\dagger}_{\mathbf{q}}\rangle$ acquire nonzero values for small $\mathbf{q}$. (In taking the limit, $\mathbf{k+q}$ and $\mathbf{k}$ should be on opposite sides of the Fermi surface; the limit $\mathbf{q}\to 0$ of $\langle c^{\dagger}_{\mathbf{k+q},\sigma} c_{\mathbf{k},\sigma}\rangle$ is not the particle density at $\mathbf{k}$.) The self-consistency equations are derived in a mean-field approximation as follows. By a mean-field decomposition and minimization of the effective Hamiltonian Eq. (44),

$$\langle b_{\mathbf{q}}\rangle = -{\sum_{\mathbf{k}\sigma}}' \frac{\gamma(\mathbf{k},\mathbf{k+q})}{2\Omega_{\mathbf{q}}} \langle c^{\dagger}_{\mathbf{k+q}\sigma} c_{\mathbf{k}\sigma}\rangle. \tag{49}$$

The restriction on the sum indicates that the sum is over states within ω_c of the chemical potential and that the states $\mathbf{k},\mathbf{k+q}$ refer to (occupied, unoccupied) states, or vice versa.

The effective *mean-field* Hamiltonian for the electrons is now

$$\begin{aligned} H_{eff} &= \sum_{\mathbf{k}\sigma} \epsilon_{\mathbf{k}} c^{\dagger}_{\mathbf{k}\sigma} c_{\mathbf{k}\sigma} + {\sum_{\mathbf{k},\mathbf{q}\sigma}}' V(\mathbf{k},\mathbf{k+q}) c^{\dagger}_{\mathbf{k+q}\sigma} c_{\mathbf{k}\sigma} \\ &\equiv \sum_{\mathbf{k}\sigma} E_{\mathbf{k}} \tilde{c}^{\dagger}_{\mathbf{k}\sigma} \tilde{c}_{\mathbf{k}\sigma}, \end{aligned} \tag{50}$$

$$V(\mathbf{k},\mathbf{k+q}) \equiv \gamma(\mathbf{k},\mathbf{k+q})(\langle b_{\mathbf{q}}\rangle + \langle b^{\dagger}_{-\mathbf{q}}\rangle). \tag{51}$$

One may write H_{eff} in real space as a tight binding Hamiltonian on the lattice,

$$H_{eff} = \sum_{\mathbf{R}_i,\mathbf{R}_j\sigma} t(\mathbf{R}_i,\mathbf{R}_j) c^{\dagger}_{i\sigma} c_{j\sigma}, \tag{52}$$

which shows effective long-range, angle-dependent hopping, which is to be determined self-consistently.

The one-particle Green's function for H_{eff} in the self-consistent Brillouin-Wigner approximation has a self-energy that is an infinite continued fraction which may be summed formally to give the one-particle propagator

$$G(\mathbf{k},\omega) = \frac{1}{\omega - \epsilon_{\mathbf{k}} - D(\mathbf{k},\omega)}, \tag{53}$$

where

$$D(\mathbf{k},\omega) = {\sum_{\mathbf{q}}}' \frac{|V(\mathbf{k},\mathbf{k+q})|^2}{\omega - \epsilon_{\mathbf{k+q}} - D(\mathbf{k+q},\omega)}. \tag{54}$$

On the energy shell, at

$$\omega = E_{\mathbf{k}} = \epsilon_{\mathbf{k}} + D(\mathbf{k},E_{\mathbf{k}}), \tag{55}$$

$$D(\mathbf{k},E_{\mathbf{k}}) = {\sum_{\mathbf{q}}}' \frac{[f(E_{\mathbf{k+q}}) - f(E_{\mathbf{k}})]|V(\mathbf{k},\mathbf{k+q})|^2}{E_{\mathbf{k+q}} - E_{\mathbf{k}}}. \tag{56}$$

This formal solution to Eq. (50) is exact in the limit that the number of states $(\mathbf{k+q})$ coupled to a given state $\mathbf{k}$ is very large compared to 1. It also follows by taking the expectation value of (50) in the new state that

$$D(\mathbf{k},E_{\mathbf{k}}) = \sum_{\mathbf{q}} V(\mathbf{k},\mathbf{k+q}) \langle c^{\dagger}_{\mathbf{k+q}} c_{\mathbf{k}}\rangle. \tag{57}$$

Comparing Eqs. (56) and (57) and using Eq. (51),

$$\langle c^{\dagger}_{\mathbf{k+q}} c_{\mathbf{k}}\rangle = \frac{\gamma(\mathbf{k},\mathbf{k+q})[f(E_{\mathbf{k+q}}) - f(E_{\mathbf{k}})](\langle b_{\mathbf{q}}\rangle + \langle b^{\dagger}_{-\mathbf{q}}\rangle}{E_{\mathbf{k+q}} - E_{\mathbf{k}}}. \tag{58}$$

Inserting $\langle b_{\mathbf{q}}\rangle, \langle b^{\dagger}_{-\mathbf{q}}\rangle$ from Eq. (49) and after a simple manipulation I obtain the self-consistency condition

$$\begin{aligned} V(\mathbf{k+q}/2,\mathbf{k-q}/2) = {\sum_{\mathbf{k}'}}' g(\mathbf{k},\mathbf{k}') &\frac{f(E_{\mathbf{k}'+\mathbf{q}/2}) - f(E_{\mathbf{k}'-\mathbf{q}/2})}{(E_{\mathbf{k}'+\mathbf{q}/2} - E_{\mathbf{k}'-\mathbf{q}/2})} \\ &\times V(\mathbf{k}'+\mathbf{q}/2,\mathbf{k}'-\mathbf{q}/2). \end{aligned} \tag{59}$$

In Eq. (59), the sum is restricted to states $\mathbf{k}'$ such that $\epsilon(\mathbf{k}')$ is within about Ω_0 of the chemical potential μ, as required by the retarded nature of the fermion-boson interaction.

Note that we have already proven in Eq. (55) that the quasiparticle energies in the new state obey

$$E_{\mathbf{k}\sigma} = \epsilon_{\mathbf{k}\sigma} + D_{\mathbf{k}\sigma}. \tag{60}$$

There is no self-energy in quadrature as in the BCS theory or the theory of charge- and spin-density waves. This of course has pronounced effects on the spectroscopic and thermodynamic properties in the new state.

C. Solution near T_g

The self-consistent solution of Eqs. (56), (58), and (59) is a complicated problem which however simplifies in the "Ginzburg-Landau" regime which provides the transition temperature and the leading temperature dependence of the gap below it. In this regime only very small-$\mathbf{q}$ old states are admixed to a given $\mathbf{k}$ in the new states. I will assume that the solution obtained continues qualitatively to lower temperatures.

In this regime, note first that since $g(\mathbf{k},\mathbf{k}')$ is proportional to $\gamma(\mathbf{k})\gamma(\mathbf{k}')$ for $q\to 0$, $V(\mathbf{k},k+q)\sim\gamma(\mathbf{k})$ also. Second, $E(k)\approx\epsilon(k)$ for $|\epsilon(k)-\mu|\gtrsim\Omega_0^0$. The self-consistency condition (59) may therefore be rewritten in the limit $\mathbf{q}\to\mathbf{0}$ as

$$1 = \frac{-2}{\Omega_0}\sum_{\mathbf{k}}{}' |\gamma(\mathbf{k})|^2 \left(\frac{f(E^{>}_{\mathbf{k}}) - f(E^{<}_{\mathbf{k}})}{E^{>}_{\mathbf{k}} - E^{<}_{\mathbf{k}}}\right). \tag{61}$$

Here $E^{>}_{\mathbf{k}}, E^{<}_{\mathbf{k}}$ are the new one-particle eigenvalues above and below the chemical potential, respectively. To determine $E_{\mathbf{k}}$, one must satisfy Eq. (60) in a manner continuous with the approach to the instability, where $\partial\Sigma/\partial\mathbf{k}$ diverges. Accordingly, I seek a solution with

$$E^{>}_{\mathbf{k}} = \epsilon_{\mathbf{k}} + D(\hat{k}_f),$$

$$E^{<}_{\mathbf{k}} = \epsilon_{\mathbf{k}} - D(\hat{k}_f),$$

$$(E^{>,<}_{\mathbf{k}} - \epsilon_{\mathbf{k}}) \to 0 \quad \text{for } |E^{>,<}_{\mathbf{k}} - \mu| \gg \Omega_0, \tag{62}$$

with the additional condition that $D(\hat{k}_f) \geq 0$ for all $\hat{k}_f$.

This manner of opening a gap at the chemical potential is unusual. The physics of this gap is distinct from that of the gaps of Bloch-Wilson one-electron theory, the BCS gap, the Mott gap, or the charge-density (CDW) or spin-density wave (SDW) gaps. In the mean-field approximation the gap arises due to an effective infinite-range hopping exhibited in Eq. (52).

The integral equation (61) for $D(\mathbf{k})$ may be rewritten as

$$1 = -\frac{-2}{\Omega_0}\int \frac{d\hat{k}_f}{2\pi}\frac{|\gamma(\hat{k}_f)|^2}{D(\hat{k}_f)} \times \int_0^{\omega_c} d\epsilon\, \rho_0(\epsilon)\frac{\tanh[\beta D(\hat{k}^f)]}{1+\cosh(\beta\epsilon)\cosh^{-1}[\beta D(\hat{k}^f)]}. \tag{63}$$

At temperatures for which $\beta D(\hat{k}_f) \ll 1$, Eq. (63) reduces to

$$1 - \tanh(\beta\omega_c/2)\int \frac{1}{\Omega_0}\rho(0)\frac{d\hat{k}_f}{2\pi}|\gamma(\hat{k})|^2 - \beta^2/12[\tanh(\beta\omega_c/2) - \tanh^3(\beta\omega_c/2)]\frac{1}{\Omega_0}\rho(0) \times \int \frac{d\hat{k}_f}{2\pi}|\gamma(\hat{k})|^2 D^2(\hat{k}_f). \tag{64}$$

This constitutes the microscopic derivation of a free energy of the Landau form for the instability.

It is interesting to make connection with the forward scattering parameters of Landau theory. This may be done only when the cutoff ω_c satisfies $\beta\Omega_0 \gg 1$. In that case define,

$$-\frac{1}{\Omega_0}\rho(0)\int \frac{d\hat{k}_f}{2\pi}|\gamma(\hat{k}_f)|^2 \equiv F^s_\ell/(2\ell+1), \tag{65}$$

where F^s_ℓ is the spin-symmetric Landau parameter in the ℓth "angular momentum" channel. The condition for the instability is that the left side of Eq. (64) be zero. This happens at a temperature T_ℓ below which stability is achieved with a finite value for the right side, i.e., with $D(\hat{k}, T) \neq 0$. The transition temperature in that case is

$$T_\ell \approx \frac{\omega_c}{\ln\left(\frac{F^s_\ell/(2\ell+1)}{1+F^s_\ell/(2\ell+1)}\right)}. \tag{66}$$

In our problem we must take the limit $\beta\omega_c \ll 1$ for T just below T_g, where $\Omega_0 \to 0$. Then the cutoff $\omega_c \approx \gamma_0|\epsilon|$, defined in Eq. (29). The transition temperature T'_g is then given by

$$T'_g \approx (\rho_0/2)\gamma_0|\epsilon|\int \frac{d\hat{k}_f}{2\pi}\frac{|\gamma(\hat{k}_f)|^2}{\Omega_0} \approx \left(\frac{\rho_0 V^2\gamma_0}{\bar{t}^2_{pp}/\bar{t}_{pd}}\right)(1 - T'_g/T_g). \tag{67}$$

Here the relationship, Eq. (39) between the collective mode frequencies Ω_0 and the order parameter θ has been used. Equation (67) gives $T'_g \approx T_g$ for $(\rho_0 V^2 \bar{t}_{pd}\gamma_0)/(T_g \bar{t}^2_{pp}) \gg 1$. For $\gamma_0 \approx \rho_0^{-1}$ and $x \approx 0.1$, this ratio is of $O(10^4)$. One should expect that in a better theory, the TRV instability is accompanied exactly by the instability to the anisotropic gapped state. As explained later, the mean-field theory of the TRV transition is expected to be strongly modified by fluctuations. The results for the region near the transition obtained here should only be regarded as indicative.

The value of the gap for $T < T_g$ is also given by Eq. (64):

$$\frac{\int (d\hat{k}_f/2\pi)|g\,\gamma(\hat{k})|^2 D^2(\hat{k})}{\int (d\hat{k}_f/2\pi)|\gamma(\hat{k})|^2} \approx 6T_g(T_g - T). \tag{68}$$

The angular dependence of $D(\hat{k})$ is to be found from Eq. (68), subject to the condition that $D^2(\hat{k}) > 0$ for all $\hat{k}$. A family of solutions to (68) exist, the one that must be chosen is that which minimizes the energy by considering the fourth-order terms in the free energy. This is given by $D(\hat{k})$ which has the same dependence as the kernel $|g(\hat{k}_f)|^2$,

$$D(\hat{k}) \propto |\gamma(\hat{k}_f)|^2. \tag{69}$$

Referring to Eqs. (38) and (40), in the Θ_I phase, $|g(\hat{k}_f)|^2 \propto [\cos(k_{fx}a) - \cos(k_{fy}a)]^2$. This is also true in the fluctuation regime to the Θ_{II} phase. However, there, using Eq. (44), $|g(\hat{k})|^2 \propto \sin^2(k_{fx}a/2 \pm k_{fy}a/2)$, the two signs refer to the two different reflection-symmetry-violating domains of Θ_{II}.

In the Θ_{II} phase, the most unstable mode is the mixing mode for which the coupling function again has d-wave symmetry and the gap is expected to have the shape $[\cos(\hat{k}_{fx}) - \cos(\hat{k}_{fy})]^2$.

The value of the gap is expected to grow for lower temperatures approximately as in Eq. (68). The amplitude of the gap in the one-particle spectrum at the chemical potential D_0 at $T=0$ is $\approx\sqrt{6T_g(x)}$.

One should ask at this point how the transition to the TRV symmetry is affected by the pseudogap appearing simultaneously with it. Recalling that the transition to that phase depends on admixing states between the bonding and the nonbonding bands, the effect is only of order $D_0/t_{pd} \ll 1$. It would of course be desirable to derive the TRV plus the

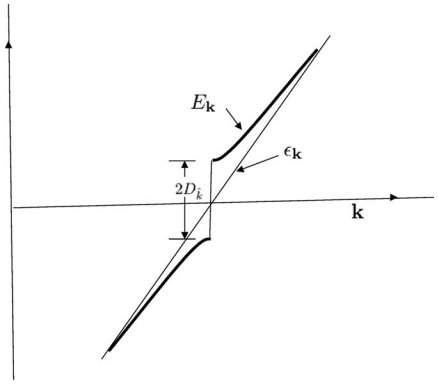

FIG. 3. The one-particle dispersion measurable by ARPES expected for the pseudogap phase. ϵ_c has been assumed to be equal to D_0, the maximum gap. The discontinuity D is a function of angle around the Fermi surface.

anisotropic gap in a single mean-field ansatz rather than with the procedure used here.

V. SOME PROPERTIES OF THE TRV PSEUDOGAP STATE

In Eq. (62), the dispersion $E_{\mathbf{k}}$ is determined for $\beta D(\hat{k}) \ll 1$. To calculate properties at intermediate and low temperatures we need $E_{\mathbf{k}}$ for $\beta D(\hat{k}) \gtrsim 1$. To meet the requirement that $E_{\mathbf{k}} \to \epsilon_{\mathbf{k}}$ for $|E_{\mathbf{k}} - \mu| \gg D(\hat{k})$, we may choose

$$E_{\mathbf{k}} = \epsilon_{\mathbf{k}} + D(\hat{k})/[1 + (\epsilon_{\mathbf{k}}/\epsilon_c)^2]. \tag{70}$$

The derivation of ϵ_c is only possible through a solution of the self-consistency equations at low temperatures together with the requirement that the number of states below the chemical potential is constant. One expects ϵ_c to be $O(D_0)$. The dispersion in Eq. (70) is represented in Fig. 3.

The density of the state in the pseduogap phase may be calculated as

$$N_p(\omega) = \sum_{\mathbf{k}} (1/\pi)\delta(\omega - E_{\mathbf{k}}). \tag{71}$$

If $\epsilon_c \gg D_0$, this can be evaluated analytically to give

$$N_p(\omega) = \begin{cases} \nu(0)\dfrac{2}{\pi}\arcsin\left(\left|\dfrac{\omega}{D}\right|^{1/2}\right), & \left|\dfrac{\omega}{D}\right| \leqslant 1, \\ \rho(0), & \left|\dfrac{\omega}{D}\right| \geqslant 1. \end{cases} \tag{72}$$

This increases as $|\omega/D|^{1/2}$ for $|\omega/D| \ll 1$. For a general ϵ_c, the asymptotic low-energy density of states keeps this form. For ϵ_c of $O(D_0)$, the density of states can only be evaluated numerically.

This density of states ignores both the effect of impurity scattering as well as lifetimes due to inelastic scattering which are a function of energy and temperature. The latter are included below in calculating the single-particle spectral function.

A. Single-particle spectral function

1. Inelastic scattering

To obtain the spectral function $A(k,\omega)$ measured by ARPES one needs besides Eq. (70) the self-energy of the single-particle states. To calculate the scattering rate, we first estimate the polarizability $\chi_0(\mathbf{k},\mathbf{q},\omega)$ from a single-particle-hole bubble formed from states $\mathbf{k}$ and $\mathbf{k}+\mathbf{q}$,

$$\mathrm{Im}\,\chi_0(\mathbf{k},\mathbf{q},\omega) \propto \sum_{\mathbf{k}} \delta(\omega - (E_{\mathbf{k}+\mathbf{q}} - E_{\mathbf{k}}))[f(E_{\mathbf{k}+\mathbf{q}}) - f(E_{\mathbf{k}})]. \tag{73}$$

We are interested especially in the low-energy contributions to $\mathrm{Im}\,\chi_0(\mathbf{q},\mathbf{k}\omega)$. These come when the initial state $\mathbf{k}$ is near a zero of the pseudogap. With such an initial state and the gap in the single-particle spectrum $D(\hat{\mathbf{q}})$, the integrals in Eq. (73) may be evaluated to yield the result that

$$\mathrm{Im}\,\chi_0(\mathbf{k},\mathbf{q},\omega) \propto \omega\Theta(\omega - D(\hat{\mathbf{q}}))/v_f^2 \tag{74}$$

with the function of the angle $\mathbf{q}$ multiplying (74) which has a weak dependence, except when $\mathbf{k}+\mathbf{q}$ is also near one of the zeros of the gap function. In that case

$$\mathrm{Im}\,\chi_0(\mathbf{k},\mathbf{q},\omega) \propto \omega/q^2\Theta(\omega - D(\hat{\mathbf{q}})). \tag{75}$$

Given that the spectral weight of fluctuations for most $(\mathbf{k},\mathbf{q})$ is 0 below an energy $D(\hat{\mathbf{q}})$ and increases only linearly beyond it, no important modifications are expected due to interactions. For $\omega \gg D(q)$, $\mathrm{Im}\,\chi_0(\mathbf{k},\mathbf{q},\omega)$ must have the same form as in the normal state for all $\mathbf{k}$, i.e., as in the marginal Fermi-liquid (MFL) hypothesis.

From the estimates above one can calculate the form of the self-energy $\Sigma(\mathbf{k},\omega)$ for $\mathbf{k}$ in the vicinity of the region of zero gap. For this calculation the region in which $\mathrm{Im}\,\chi$ is given by (75) is ignorably small. Using (74), a simple calculation gives for $\omega/D_0 \ll 1$ that

$$\mathrm{Im}\,\Sigma(\mathbf{k},\omega) \propto N(0)\omega^2/D_0. \tag{76}$$

For $\omega/D_0 \gg 1$, the self-energy must revert to the MFL form.

For a $\mathbf{k}$ away from the zero of the gap, and near energy $D(\hat{\mathbf{k}})$, no decay through an inelastic process is possible kinematically for ω less than $D(\hat{\mathbf{k}})$. (This is the process where the intermediate fermion state is near the zero of the pseudogap and the scattered polarizability makes up the momentum difference.) Therefore for $(\omega,T) \ll D(\hat{\mathbf{k}})$ the self-energy is exponentially small. For $(\omega,T) \gtrsim D(\hat{\mathbf{k}})$ it returns to the value $\Sigma_n(\omega,q,T)$ without the pseudogap. So

$$\mathrm{Im}\,\Sigma(\omega,\mathbf{k},T) \approx \mathrm{sech}\left(\frac{D(\hat{\mathbf{k}},T)}{(\omega^2 + \pi^2T^2)^{1/2}}\right)\mathrm{Im}\,\Sigma_n(\omega,\mathbf{k},T). \tag{77}$$

The spectral function at the wave vectors away from the zeros of the gap $E(\hat{k}_f) = \pm D(\hat{k}_f)$ calculated using Eq. (77) and the marginal Fermi-liquid form for Σ_n is plotted in Fig. 4 for a few temperatures. A pseudogap in the direction $\hat{k}_f$ appears below $T \approx D(\hat{k}_f)$. At zero temperature the Fermi surface is

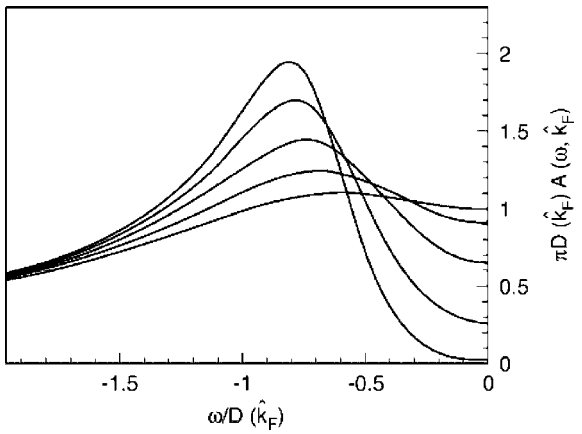

FIG. 4. Calculated spectral function in the pseudogap phase excluding linewidth due to impurity scattering. The spectral function in any given direction $\hat{k}$ has been normalized to the value of the gap in that direction, $D\hat{k}$, and the energy is also normalized to the value of the gap. The temperatures shown are given by $T=nD(\hat{k}_f)/4\pi$ for $n=1,2,\ldots,5$.

composed of four points. But at finite temperature a gap can be discerned in a direction $\hat{\mathbf{k}}_f$ only if T is less than about $D(\hat{k}_f,T)$. This produces the illusion of "Fermi arcs," which shrink as the temperature decreases.

2. Impurity scattering

It is important in the cuprates (and other layered materials) to distinguish the effect of impurities in the planes which are expected to act as point or large-angle scatterers from that of impurities in between the planes which scatter electrons in the planes only through small angles on the Fermi surface.[51] In the latter case, the scattering rate at a point $\mathbf{k}$ (calculated in the Born approximation) depends on the local density of states at the point, i.e., on the spectral function $A(\mathbf{k},\omega)$. This idea is important to understand the difference in the scattering rate deduced from single-particle spectra from that in transport, the insensitivity of T_c to small-angle scattering, the Hall effect, and the line shape as a function of ω and its variation with $\hat{k}_f$ of the spectral function $A(\mathbf{k},\omega)$ in the superconducting state.[52]

Given the form of the spectral function for the pseudogap *neglecting impurity scattering* in Fig. 4, small-angle impurity scattering also has interesting effects on the *observable* spectral function in the pseudogap state. It follows that elastic scattering will be anisotropic, increasing from the nodal region where the spectral function is small to the antinodal region, where it is large. It also follows that the small angle scattering rate will be small in the antinodal region in the tail of $A(\mathbf{k},\omega)$ toward the chemical potential and large on the other side. Such features have been observed in experiments.[16] The detailed comparison of experimental $A(\mathbf{k},\omega)$ with calculations should incorporate these effects of impurity scattering.

In the classical fluctuation regime I, above the pseduogap regime, the single-particle spectra should also show the frequency dependence calculated in Eqs. (31) and (32). Since it

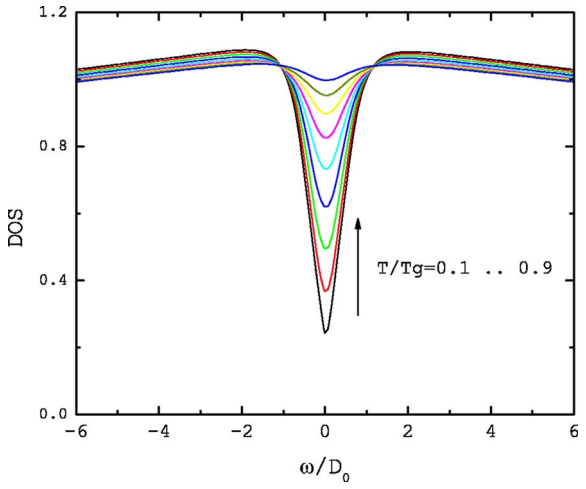

FIG. 5. (Color online) Calculated density of states in the pseudogap phase at several temperatures. D_0 is chosen as $2.5T_g$.

is only weakly dependent on ν, $|k-k_f|$, and ϵ, it may appear within the experimental uncertainty as enhanced elastic scattering, which is angle dependent $\propto|\gamma(\hat{k}_f)|^2$.

VI. COMPARISON WITH MEASURED PROPERTIES OF THE PSEUDOGAP PHASE

The effect of impurities is much less in evidence when one calculates the density of state $N_p(E)$ by integrating the spectral function over $\mathbf{k}$. The calculated $N_p(E)$, for any x at several temperatures below $T_p(x)$, is shown in Fig. 5. To compare, the measured density of states by scanning tunneling microscopy is shown in Fig. 6. I do not have anything to say about the general approximately linear variation of the density of states as a function of energy over the whole energy range, which is found both above and below T_p. If one looks at the features brought about by the pseudogap, good correspondence may be discerned in both the energy and the temperature dependence. Of special importance is to note the absence of the BCS-type singularity in the density of states

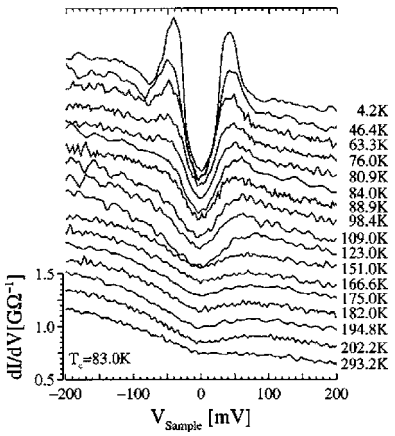

FIG. 6. Measured density of states at temperatures in the pseudogap phase obtained by Renner *et al.* (Ref. 53) in Bi-2212, by scanning tunneling microscopy.

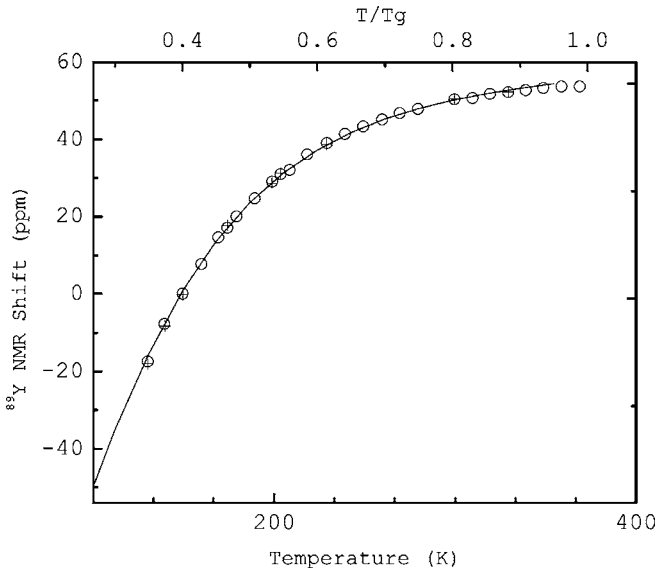

FIG. 7. Calculated magnetic susceptibility as a function of temperature compared with that deduced from Knight shift measurements reported in Fig. 3 of Ref. 62. Note that Knight shift measures both the diamagnetic and the paramagnetic susceptibility. In the comparison with the experiments, a temperature-independent diamagnetic term has been added to the calculated values.

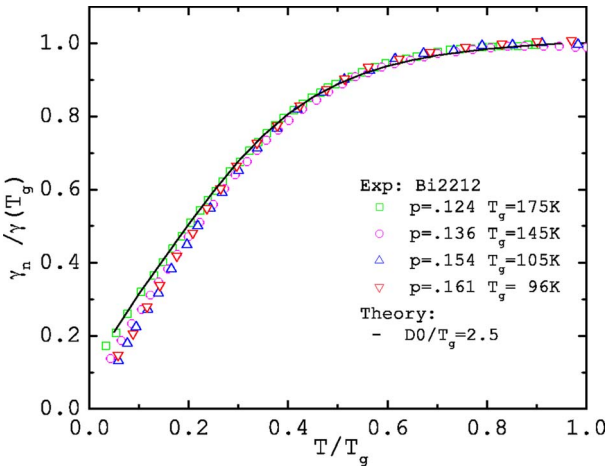

FIG. 8. (Color online) Calculated specific heat coefficient $\gamma(T)$ for various dopings x compared to the values deduced from experiments; the specific heat data are the same as extracted in Fig. 12 of Ref. 54. These authors have measured the specific heat from temperatures above T_g to well below T_c. From the measurements they extract the "normal" state specific heat below T_c by taking into consideration the condensation energy of superconductivity related to T_c using the same formula that works when there is no pseudogap.

in the pseudogap both in the calculations and in the experiments in the pseudogap regime. In the experiments it appears as one cools below $T_c(x)$. (Such singularity is present in the pseudogap region in theories based on any translational symmetry breaking, for example a charge-density wave or a D-density wave.) The variation of the pseudogap feature as a function of temperature in the calculated curves also bears close correspondence to the experiments.

The magnetic susceptibility $\chi(T)$ and the specific heat coefficient $\gamma(T) \equiv C_v/T$ at different x, calculated from the density of states of Fig. 5 are presented in Figs. 7 and 8 together with the experimental results. The temperature dependence of the measured $\chi(T)$ for a particular x is compared with experiment in Fig. 7 with $D_0/T_g=2.5$. The specific heat results in Ref. 54 for various x are rescaled with a $T_g(x)$ to lie as shown in Fig. 8 with a common ratio $D_0(x)/T_g(x)=2.5$. The values of $T_g(x)$ are within the uncertainty the same as the values where the pseudogap is seen in the specific heat or the resistivity. Considering the errors in extracting the electronic specific heat from the measured specific heat, no more sophisticated fitting is warranted, although clearly the fitting could be further improved by choosing a slightly varying $D_o/T_g(x)$ for different x.

Within the uncertainties in the determination, the experimental $C_v(T,x)/T\chi(T,x)$ is independent of temperature,[7] in agreement with the result here. The agreement of the calculated thermodynamics with the experiments should give one confidence in the underlying theoretical ideas.

From Eq. (72), it follows that the low-temperature specific heat C_v is predicted to be $\sim T^{3/2}$ and magnetic susceptibility $\chi \sim T^{1/2}$. Due to the intervention of superconductivity, it is hard to test these power laws accurately. One can deduce the continuation to the T dependence below T_c of $C_v(T)$ by invoking conservation of entropy on the available measurements and the $T=0$ limit. $C_v(T) \sim T^{3/2}$ for $T \ll T_x$ is then not inconsistent while $C_v(T) \sim T$ clearly is inconsistent. The temperature dependence of C_v in the pseudogap regime implies that the temperature dependence and magnitude of superfluid density ρ_s in the pseudogap regime are quite different from usual. This is a subject for further investigations.

VII. CONCLUDING REMARKS

This work rests on the development of two ideas using very elementary methods: that time-reversal-violating states occur in a metal due to large finite-range interactions and that such states necessarily have anisotropic gaps at the chemical potential. It is suggested that these determine the properties of region II of the phase diagram ending at the putative QCP, which is the basis for the singular fluctuations responsible for the properties in region I and the glue for superconductive pairing. The claim that this investigation provides the basic framework for a microscopic theory of the cuprates can only be made if the unusual predictions made are further confirmed and verified. I also discuss in this section the shortcomings of the mean-field theory in this paper in relation to the properties of the cuprates.

A. Predictions

Two classes of verifiable predictions have been made in this and related work: (a) The pseudogap state violates time reversal without altering the translational symmetry and ends at a QCP inside the superconducting dome of compositions; and (b) the specific features of the dispersion and the resulting thermodynamic properties in the pseudogap state.

Concerning (a), the most dramatic prediction, as has been mentioned, has been verified[11] through specially designed ARPES experiments with polarized photons. The symmetry of the TRV state is consistent with the Θ_{II} state. An important part of the verified prediction is that the magnitude of the measured time-reversal violation in a given direction in the Brillouin zone is the same for all states in the conduction band measured[11] (in an energy range of about 0.4 eV below the chemical potential). According to the theory, these should all be given by the parameter θ.

These results need to be confirmed independently with other techniques, preferably more direct; also more compounds with a range of compositions need to be measured. Experiments using other techniques[29,30] have been proposed to test for time-reversal invariance and the specific point-group symmetry proposed for the current patterns. An especially notable prediction[30] is the nature of the superconducting state for compositions in which the pseudogap occurs in the normal state. This can be verified through experiments related to the Josephson effect. (A direct test has come recently through polarized neutron diffraction experiments.[12])

Several confirmations of the prediction that the pseudogap state ends at a QCP inside the superconducting dome now exist through tunneling[9] and transport[10,55] experiments in a magnetic field.

Concerning (b), the principal predictions are as follows. (i) The dispersion of quasiparticles in the pseudogap state near the gap edge has the form given by Eq. (70) and exhibited in Fig. 3. To check this the spectral function including the self-energy must to be used to deduce the quasiparticle dispersion. (ii) The dispersion has point-group symmetry in a single domain given by Eqs. (A8) and (A9) of the Appendix. (iii) The specific heat and the magnetic susceptibility at very low temperatures in the pseduogap state have the temperature dependence discussed above. The specific heat (and the related experiment of thermal conductivity) need to be done in a high enough magnetic field to suppress superconductivity.

A very important issue is the specific heat at the onset of the pseudogap. As discussed below the transition may not have a singularity in the specific heat. But there is no reason why there should not be a bump. The deduction of the electronic specific heat through subtraction of the lattice heat capacity by comparison between samples for temperatures above 40 K (where it is less than 1% of the total) is not accurate enough to decipher bumps. Measurements at much lower temperatures are required which must be done in a large enough field to suppress superconductivity with the transition to the pseudogap preserved.

It is obvious that the fluctuation spectra of the form of Eq. (1) observed in the region I of the phase diagram at long wavelengths by Raman scattering should be modified in the classical fluctuation regime qualitatively as in Eq. (29). This is consistent with some recent observations.[56] The detailed behavior can only be predicted by a proper theory in the fluctuation regime (see below) and not be a mean-field theory supplemented by Gaussian fluctuations as in this paper. The result derived here that the fluctuations occur in specific IR's given by the coupling of the fluctuation vertex to the fermions is likely to survive since it is based on symmetry only.

B. Specific heat near the transition

A difficulty in regarding the pseduogap region as a distinct phase is that there is no singularity in the specific heat at the temperature where it begins to be observed in many other experiments. In this connection, it is worthwhile looking at the statistical mechanics for a TRV transition into the Θ_{II} phase. This phase breaks both time reversal and inversion. A statistical mechanical model describing the transition to such a phase is that of the two-coupled Ising model. A realization of the model is the (anisotropic) Ashkin-Teller model:

$$H = -J\sum_{\langle ij\rangle}[(\mu_i\mu_j + \lambda_i\lambda_j) + y(\mu_i\mu_j\lambda_i\lambda_j)] \tag{78}$$

where the sum covers nearest neighbors on a lattice. For $-1 < y < 1$, the model in two dimensions has a line of critical points with variable critical exponents. [The model deduced in this paper starting from fermions and interactions as in Eqs. (9)–(11) gives the model with $y=0$.] We may identify $\langle\mu\rangle$ as the time-reversal order parameter and $\langle\lambda\rangle$ as the inversion-breaking order parameter. J, y are positive in our problem signifying *ferromagnetic* alignment of $\langle\mu\rangle, \langle\lambda\rangle$ as well as of $\langle\mu\lambda\rangle$. In this case the specific heat exponent α varies from 0 to $-2/3$ as y varies from 0 to 1, i.e., the specific heat has no divergence.[57]

The specific heat is part of the general problem of deriving the fluctuation spectra at the TRV-pseudogap transition in the classical regime as well as in the quasiclassical regime (i.e., region I in the phase diagram of Fig. 1), which leads to MFL properties as well as providing the glue for pairing. In this connection, it is worth noting that the Ashkin-Teller model has interesting topological excitations. These may well be relevant to deriving Eq. (1).

C. Alternate theories of the pseudogap

The theories to explain the pseudogap phenomena can be broadly divided into two categories: those that do not have a quantum critical point which marks the end point of a broken symmetry and those like the one presented here that do. In the former are various versions of resonating valence-bond theory[58] and those based on the idea that the pseudogap is due to the fluctuations towards the d-wave superconducting state.[59] This category of theories can be excluded if a quantum critical point for x in the superconducting dome exists. Extensive evidence for a quantum critical point within the region in x in which superconductivity occurs may be found, the most obvious is the linear temperature dependence of resistivity down to the lowest temperature in all cuprates in a narrowing composition range as temperature is decreased up to the temperature where superconductivity intervenes. In one case, this is known by suppression of superconductivity by a magnetic field down to 40 mK (Ref. 60) and in another[61] down to 2 K. Such a linear resistivity is not possible without fluctuations persisting unchanged in spectral strength down to energies lower than the temperature of measurements. Moreover I am not aware of any theory based on the absence of broken symmetry which has succeeded in calculating the single-particle spectra or the specific heat and

magnetic susceptibility such as presented here.

There are two other theories[38,39] besides that presented here which rely on a broken symmetry and a quantum critical point. The first relies on a charge-density wave and the second (DDW) on a time-reversal-breaking phase which also breaks translational symmetry. There is no evidence for a charge-density wave and associated structural transition setting in at the pseudogap temperature in any cuprate. These should be easy to detect were they to occur, since the characteristic free energy associated with the pseudogap phase is a few hundred degrees per unit cell. Both a CDW and DDW would lead to a Fermi surface with pockets due to the change in the Brillouin zone. No evidence in ARPES of such Fermi-surface reconstruction is found. Moreover, as discussed earlier the density of states with translational symmetry breaking has characteristic singularities at the edges of the (maximum) gap which are not seen in tunneling measurements.

Despite the agreements with experiment for the present theory noted earlier, its fate rests on whether the experiments[11,12] which are consistent with the predicted broken symmetry are correct.

D. Shortcomings

Some major blank spaces in the picture have already been mentioned; some others ought to be mentioned. The most important of these is the derivation of the phenomenological Eq. (1) and superconductivity. The fluctuation spectrum of Eq. (1) has the right energy scale and coupling constant (both deduced from experiments) to give the right scale of superconducting transition temperatures. The developments in this paper identify the nature of the fluctuations to be time-reversal and chirality fluctuations which condense to give the pseudogap region of the phase diagram.

The major issue of principle about superconductivity is how a (nearly) momentum-independent fluctuation spectra, which predicts the observed momentum-independent single-particle self-energy, can lead to d-wave superconductivity. The answer lies in the momentum dependence of the coupling functions of the current fluctuations to the fermions. As noted earlier, the spectrum of Eq. (1) acquires a dependence on the internal momentum $\mathbf{k}$ of the particle-holes to represent the IR of the fluctuation spectra. In a separate paper, I show that this leads to a momentum independent self-energy but a momentum-dependent pairing vertex.

Some other issues worth investigating are the competition between the pseudogap state investigated here and the antiferromagnetic state near half filling, the transport properties in the pseudogap state and the derivation of the unusual superfluid density in the pseudogap state. A complete solution of the self-consistency equations in Sec. IV B is also desirable. Many of these issues which involve detailed calculations are worth the effort only if the principal results of this paper are verified by experiments.

ACKNOWLEDGMENTS

I am grateful to Lijun Zhu for the comparison with experimental data shown in Figs. 4–7. I have also benefited enormously from conversations with so large an array of experimentalists and fellow theorists that they cannot all be mentioned here. Special acknowledgements are due to Vivek Aji, Adam Kaminski, Elihu Abrahams, and Peter Woelfle. Part of this work was done at Bell laboratories and part of the manuscript written at Aspen Center for Physics and during visits to Institute for Condensed Matter Physics at University of Karlsruhe.

APPENDIX

1. Calculation of energies

To determine the mean-field value of the order parameter, the dependence of the energy of the states of the conduction band on the invariant flux $\Phi(\mathbf{k}) \equiv \theta_x(\mathbf{k}) - \theta_y(\mathbf{k})$ is calculated. To do this in general, the 3×3 matrix Eq. (17) or (21) needs to be diagonalized. This leads to a rather messy expression. Answers with the correct symmetry may be obtained by calculating the energy perturbatively in t_{pp}/t_{pd}. Actually, this parameter may be no smaller than about $1/2$. Treating it as small has the advantage of obtaining results analytically and no disadvantage as far as the qualitative validity of the results is concerned. The change in energy of the conduction band is

$$\delta\epsilon_{c\mathbf{k}} \approx -4\bar{t}_{pp}\frac{s_x^2 s_y^2}{s_{xy}^2}\cos[\theta_x(\mathbf{k}) - \theta_y(\mathbf{k})]. \tag{A1}$$

$\theta_{x,y}(\mathbf{k})$ for the Θ_I and Θ_{II} phases are given by Eqs. (18) and (19). $R_{I,II}$ and $\phi_{I,II}$ are to be determined variationally. (There arise terms in the calculation of the energy which do not depend on both $R_{I,II}$ and $\phi_{I,II}$. These are properly ignored in the results given below.)

We write here the mean-field energy which is dependent on the order parameter up to order $\left(\frac{R}{\bar{t}_{pd}}\right)^4$. For the Θ_I phase

$$\begin{aligned}\delta F(R_I,\phi_I) \approx \frac{R_I^2}{V} - 2\sum_{\mathbf{k}}[1-f(\epsilon_{c\mathbf{k}})]\bar{t}_{pp} \\ \times\left[\left(\frac{R_I}{2\bar{t}_{pd}}\right)^2(\sin^2\phi_I) \right. \\ \left. -\frac{1}{12}\left(\frac{R_I}{2\bar{t}_{pd}}\right)^4(\sin^4\phi_I)\right]\frac{s_x^2 s_y^2}{s_{xy}^2}.\end{aligned} \tag{A2}$$

For the Θ_{II} phase,

$$\begin{aligned}\delta F(R_{II},\phi_{II}) \approx \frac{R_{II}^2}{V} - 2\sum_{\mathbf{k}}[1-f(\epsilon_{c\mathbf{k}})]\bar{t}_{pp} \\ \times\left[\left(\frac{R_{II}}{2\bar{t}_{pd}}\right)^2(\sin^2\phi_{II}) - \frac{1}{12}\left(\frac{R_{II}}{2\bar{t}_{pd}}\right)^4(\sin^4\phi_{II})\right] \\ \times\frac{s_x^2 s_y^2}{s_{xy}^2}\left(\frac{s_x c_y \pm c_x s_y}{s_{xy}^2}\right)^2.\end{aligned} \tag{A3}$$

Compare the coefficients of the $(R/t_{pd})^2$ terms in Eqs. (A2) and (A3). Only the last factor in the parentheses is different and the rest of the term is negative at each point

(k_x, k_y). Then it is easy to see that the energy of the state Θ_{II} is always lower than of the Θ_I phase such that for fixed parameters the transition temperature to the former is larger than the latter. Although this is true in the simplest model interactions, it may not be generally true.

On minimizing, ϕ_0 is $\pm\pi/2$ for either phase. Also $R_0 \neq 0$ at $T=0$ for the Θ_{II} phase only if

$$\frac{\bar{t}_{pd}^2}{V} < \sum_{\mathbf{k}>\mathbf{k}_f} \frac{2\bar{t}_{pp}^2 s_x^2(k) s_y^2(k)}{\epsilon_{\mathbf{k}}^0 s_{xy}^4(k)} (s_x c_y \pm s_y c_x)^2. \tag{A4}$$

For $\epsilon_d \neq 0$, $\bar{t}_{pd}^2 s_{xy}^2$ is replaced approximately by $\bar{t}_1^2 s_{xy}^2 + \epsilon_d^2$.

For the Θ_I phase the same condition gives a minimum value of V larger by a numerical factor of $O(1)$ with the other parameters fixed.

Note that the x dependence occurs through that of $\bar{t}_{pd}$ and $\bar{t}_{pp}$ besides the Fermi energy. Equation (A4) is satisfied only for x, the deviation of doping from half filling, less than a critical doping $|x_c|$. This may be estimated from the integral in Eq. (A4); the critical doping at $T=0$ is

$$x_c \approx V\bar{t}_{pp}/(2\bar{t}_{pd}^2 \pm V\bar{t}_{pp}). \tag{A5}$$

Here the plus sign is for the deviation of electron density and minus sign for the deviation of hole density from half filling.

Similarly the value of the order parameter at $T=0$ may be estimated from the energy expanded to order (R_0^4) to be

$$\theta_0 \equiv \langle R \rangle / 2\bar{t}_{pd} \approx x_c |x_c - x|^{1/2}. \tag{A6}$$

The transition temperature T_c for a fixed x can be estimated from Eqs. (A2) and (A3). The condition obtained can be written in terms of $|x_c - x|$ and is given in Eq. (24).

The numerical coefficients in all the equations above are quite approximately determined. The aim here is to show only their dependence on the parameters of the model.

2. Energy of fluctuations

The energy of uniform fluctuations of ϕ about $\phi_0 = \pm\pi/2$ can be calculated from Eqs. (A2) and (A3) and is given, for example, in the Θ_I phase by

$$\Omega_{0,\phi} \approx \bar{t}_{pp}\theta_1^2 \sum_{\mathbf{k}} 2\frac{s_x^4 s_y^4}{s_{xy}^4}, \tag{A7}$$

which is of $O(\theta_0^2 \bar{t}_{pp})$.

In a given domain of the Θ_{II} phase, with reflection symmetry broken about either $k_x=0$ or $k_y=0$ planes, the characteristic energy of oscillations to the other domain may also be estimated similarly. In Sec. IV, I have called such fluctuations the mixing fluctuations. Their energy at long wavelengths can be calculated by allowing the order parameter to be a mixture of the two domains in the mean-field calculations and picking up the coefficient of the quadratic term $(\delta\theta_m)^2$ in the mixing:

$$\sin\Phi(\mathbf{k}) = \Phi_0(c_x/s_x + c_y/s_y) + \delta\theta_m(c_x/s_x - c_y/s_y). \tag{A8}$$

The fluctuation energy proportional to $(\delta\theta_m)^2$ is

$$\Omega_{0,m} \approx \bar{t}_{pp}\theta_2^2 \sum_{\mathbf{k}} 2\frac{s_x^2 s_y^2}{s_{xy}^4}\{\sin^2[(k_x - k_y)a/2]\cos^2[(k_x + k_y)a]\}. \tag{A9}$$

This fluctuation energy is seen to be small than that of the mode of the phase of time reversal, $\delta\phi$, by about a factor of 2. The fluctuation energy for the amplitude mode can be shown to be the largest of the frequencies of the three modes.

[1] J. G. Bednorz and K. A. Mueller, Z. Phys. B: Condens. Matter **64**, 189 (1986).

[2] See, for instance, *Proceedings of the Triannual Conference on Materials and Mechanisms of Superconductivity: High Temperature Superconductors VII —M2SRIO Rio de Janeiro, Brazil, 2003*, edited by W. Ortiz, E. Mello, E. Granato, and Elisa Baggio Saitovitch [Physica C **408-410** (2004)].

[3] T. Timusk and B. W. Statt, Rep. Prog. Phys. **62**, 61 (1999).

[4] C. M. Varma, Phys. Rev. B **55**, 14554 (1997).

[5] C. M. Varma, Phys. Rev. Lett. **83**, 3538 (1999).

[6] Several calculational errors in Ref. 5 are corrected in the present paper.

[7] J. L. Tallon and J. W. Loram, Physica C **349**, 53 (2000).

[8] S. H. Naqib, J. R. Cooper, J. L. Tallon, and C. Panagopoulos, Physica C **387**, 365 (2003); S. H. Naqib, J. R. Cooper, J. L. Tallon, R. S. Islam, and R. A. Chakalov, Phys. Rev. B **71**, 054502 (2005).

[9] L. Alff *et al.*, Nature (London) **422**, 698 (2003).

[10] Y. Dagan, M. M. Qazilbash, C. P. Hill, V. N. Kulkarni, and R. L. Greene, Phys. Rev. Lett. **92**, 167001 (2004).

[11] A. Kaminski *et al.*, Nature (London) **416**, 610 (2002).

[12] B. Fauque *et al.*, cond-mat/0509210 (unpublished).

[13] C. M. Varma, P. B. Littlewood, S. Schmitt-Rink, E. Abrahams, and A. E. Ruckenstein, Phys. Rev. Lett. **63**, 1996 (1989).

[14] T. Valla, A. V. Fedorov, P. D. Johnson, Q. Li, G. D. Gu, and N. Koshizuka, Phys. Rev. Lett. **85**, 828 (2000).

[15] E. Abrahams and C. M. Varma, Proc. Natl. Acad. Sci. U.S.A. **97**, 5714 (2000).

[16] A. Kaminski *et al.*, Phys. Rev. B **71**, 014517 (2005).

[17] M. Eschrig and M. R. Norman Phys. Rev. B **67**, 144503 (2003). In this paper an approximate inversion of the ARPES data in the superconducting state at low T is performed to deduce the spectrum of the pairing glue. An angle-averaged fluctuation spectrum $\langle \alpha^2 F(\omega) \rangle$ is deduced. Most of the spectral weight comes from a broad spectrum consistent with Eq. (1). There is a diminution of that spectrum below 2Δ, as expected for a spectrum of electronic fluctuations, together with an enhancement near 2Δ. Near T_c, where $\Delta \approx 0$, the spectrum should be precisely of the form of Eq. (1). A more precise method of inverting the data, suitable for anisotropic superconductors, has been suggested by I. Vekhter and C. M. Varma, Phys. Rev. Lett., **90**, 237003 (2003).

[18] S. Sachdev, *Quantum Phase Transitions* (Cambridge University Press, Cambridge, U.K., 1999).

[19] C. M. Varma, Z. Nussinov, and W. van Saarloos, Phys. Rep. **361**,

267 (2002).
[20] H. Ding *et al.*, Nature (London) **382**, 51 (1996); A. G. Loeser *et al.*, Science **285**, 325 (1996).
[21] H. Alloul, T. Ohno, and P. Mendels, Phys. Rev. Lett. **63**, 1700 (1989).
[22] J. W. Loram *et al.*, Phys. Rev. Lett. **71**, 1740 (1993).
[23] F. Slakey, M. V. Klein, J. P. Rice, and D. M. Ginsberg, Phys. Rev. B **43**, 3764 (1991). This reference presents results in Y(123). Similar results are found down to T_c in regime I in all cuprates studied.
[24] T. Zhou *et al.*, Solid State Commun. **99**, 669 (1996).
[25] The Raman spectrum measures the response functions as a function of frequency at long wavelengths of second-rank tensors which transform as the IR's of the point group of the lattice: $A1g$, $A2g$, $B1g$, $B2g$, etc., for a square lattice. I refer to the time-reversal-breaking operators in such representations also as currents. The term is more commonly used only for the odd-symmetry channels which are measured in conductivity experiments.
[26] This is of course not uniquely determined by the experiment. One could, for example, envisage a stress-tensor component fulfilling these requirements, but it would then couple linearly to elastic constants giving thereby an anomaly in a transverse velocity or in an optical mode frequency. No such anomalies have been reported.
[27] C. M. Varma, S. Schmitt-Rink, and E. Abrahams, Solid State Commun. **62**, 681 (1987); C. M. Varma and T. Giamarchi, in *Strongly Interacting Fermions and High T_c Superconductivity*, Les Houches, Session LVI, 1991, edited by B. Doucot and J. Zinn-Justin (Elsevier Science, Amsterdam, 1995).
[28] C. M. Varma, Phys. Rev. B **61**, R3804 (2000); M. E. Simon and C. M. Varma, Phys. Rev. Lett. **89**, 247003 (2002).
[29] S. Di Matteo and C. M. Varma, Phys. Rev. B **67**, 134502 (2003); M. E. Simon and C. M. Varma, *ibid.* **67**, 054511 (2003).
[30] T. K. Ng and C. M. Varma, Phys. Rev. B **70**, 054514 (2004).
[31] J. C. Campuzano, M. Norman, and M. Randeria, in *Physics of Superconductors*, edited by K. H. Bennemann and J. B. Ketterson (Springer, Berlin, 2004), Vol. II, pp. 167–273.
[32] J. Zaanen, G. A. Sawatzky, and J. W. Allen, Phys. Rev. Lett. **55**, 418 (1985).
[33] P. W. Anderson, in *Strong Correlations and Superconductivity*, edited by H. Fukuyama, S. Maekawa, and A. P. Maozemoff (Springer, Tokyo, 1989).
[34] The effect of large repulsions can be expressed approximately as a modification of the kinetic energy by a number of methods. To my knowledge, this first appeared through Hubbard-decoupling methods in C. M. Varma and Y. Yafet, Phys. Rev. B **13**, 2950 (1976). The most popular way to realize this is the slave boson method; see, for example, N. Read and D. M. Newns, J. Phys. C **16**, 3273 (1983).
[35] C. Sire, C. M. Varma, A. E. Ruckenstein, and T. Giamarchi, Phys. Rev. Lett. **72**, 2478 (1994).
[36] I. E. Perakis, C. M. Varma, and A. E. Ruckenstein, Phys. Rev. Lett. **70**, 3467 (1993).
[37] I. Affleck and J. B. Marston, Phys. Rev. B **37**, 3774 (1988).
[38] S. Chakravarty, R. B. Laughlin, D. K. Morr, and C. Nayak, Phys. Rev. B **63**, 094503 (2001).
[39] C. Castellani, C. Di Castro, and M. Grilli, Phys. Rev. Lett. **75**, 4650 (1995).
[40] M. Grilli, R. Raimondi, C. Castellani, C. Di Castro, and G. Kotliar, Phys. Rev. Lett. **67**, 259 (1991).
[41] P. B. Littlewood, Phys. Rev. B **42**, 10075 (1990).
[42] See, for example, M. E. Peskin and D. V. Schroeder, *An Introduction to Quantum Field Theory* (Addison-Wesley, Reading, MA, 1995).
[43] R. R. Birss, *Symmetry and Magnetism* (North-Holland, Amsterdam, 1964).
[44] L. D. Landau, E. M. Lifshitz, and L. P. Pitaevskii, *Electrodynamics of Continuous Media*, 2nd ed. (Butterworth-Heinemann, Oxford, 1984).
[45] There is also an experiment that came to the opposite conclusion: S. Borisenko, A. A. Kordyuk, A. Koitzsch, T. K. Kim, K. A. Nenkov, M. Knupter, J. Fink, C. Grazioli, S. Turchini, and H. Berger, Phys. Rev. Lett. **92**, 207001 (2004); Doubts about the validity of the procedure and the incomplete nature of the experiment (for example, even the temperature of occurrence of the pseudogap in the samples studied is not determined) are expressed by J. Campuzano *et al.*, cond-mat/0309402 (unpublished).
[46] R. P. Kaur and D. F. Agterberg, Phys. Rev. B **68**, 100506(R) (2003).
[47] X. G. Wen, F. Wilczek, and A. Zee, Phys. Rev. B **39**, 11413 (1989); P. B. Wiegmann, Phys. Rev. Lett. **60**, 821 (1988).
[48] P. C. Hohenberg and B. I. Halperin, Rev. Mod. Phys. **49**, 435 (1977).
[49] C. M. Varma, cond-mat/0311145 (unpublished); Philos. Mag. **85**, 1656 (2005).
[50] See for example, D. Pines and P. Nozieres, *The Theory of Quantum Liquids* (Benjamin, New York, 1966), Sec. 1.7.
[51] E. Abrahams and C. M. Varma, Proc. Natl. Acad. Sci. U.S.A. **97**, 5714 (2000); Phys. Rev. B **68**, 094502 (2003); C. M. Varma and E. Abrahams, Phys. Rev. Lett. **86**, 4652 (2001); **88**, 139903(E) (2002).
[52] L. Zhu, P. J. Hirschfeld, and D. J. Scalapino, Phys. Rev. B **70**, 214503 (2004).
[53] Ch. Renner, B. Revaz, J.-Y. Genoud, K. Kadowaki, and O. Fischer, Phys. Rev. Lett. **80**, 149 (1998).
[54] J. W. Loram *et al.*, J. Phys. Chem. Solids **62**, 59 (2001).
[55] Y. H. Kim and G. Boebinger (unpublished).
[56] The relevant Raman results are quoted by S. Caprara *et al.*, cond-mat/0501671 (unpublished).
[57] See, for example, M. Kohmoto, M. den Nijs, and L. P. Kadanoff, Phys. Rev. B **24**, 5229 (1981).
[58] B. Wuyts, V. V. Moshchalkov, and Y. Bruynsradede, Phys. Rev. B **53**, 9418 (1996); B. Batlogg and C. M. Varma, Phys. World **13**, 33 (2000).
[59] P. Fournier, P. Mohanty, E. Maiser, S. Darzens, T. Venkatesan, C. J. Lobb, G. Czjzek, P. A. Webb, and R. L. Greene, Phys. Rev. Lett. **81**, 4720 (1998).
[60] P. W. Anderson *et al.*, J. Phys.: Condens. Matter **16**, R755 (2004).
[61] V. J. Emery and S. Kivelson, Nature (London) **374**, 434 (1995).
[62] G. V. M. Williams, J. L. Tallon, J. W. Quilty, H. J. Trodahl, and N. E. Flower, Phys. Rev. Lett. **80**, 377 (1998).